Cellulose (2025) 32:1937–1958
https://doi.org/10.1007/s10570-024-06346-1

ORIGINAL RESEARCH

Superhydrophilic self-cleaning cotton fabric with enhanced antibacterial and UV protection properties

Esfandiar Pakdel · Walid A. Daoud · Sima Kashi · Mazeyar Parvinzadeh Gashti · Xungai Wang

Received: 19 August 2024 / Accepted: 17 December 2024 / Published online: 30 December 2024

Abstract A multifunctional cotton fabric with superior photocatalytic self-cleaning, antibacterial activity and UV protection was prepared through treatment with TiO_2/Pt/SiO_2 colloid, clarifying the influence of coating formulation on these functionalities. The photocatalytic activity of coated fabrics under UV and white-fluorescent light was tested and synergistic effects of Pt and silica in enhancing the self-cleaning property of fabrics were demonstrated. Various molar ratios of Pt:Ti (0.01%, 0.1%, 0.5%, and 1%) and Ti:Si (50/50 and 30/70) were utilised in synthesising the colloids. The self-cleaning performance of fabrics was assessed through monitoring coffee stain removal efficiency and methylene blue (MB) dye degradation kinetics. The results demonstrated an effective photocatalytic self-cleaning property on fabrics coated with TiO_2/Pt/SiO_2 colloids. Increasing the concentrations of Pt and silica both contributed to enhancing the self-cleaning property. The fabric coated with ternary TiO_2/Pt/SiO_2 30/1/70 colloid resulted in 43.5% higher MB dye removal compared with pure TiO_2 after 3h irradiation under visible light. Moreover, the fabrics containing Pt 1% dopant possessed excellent bactericidal activity against both *Escherichia coli (E. coli)* and *Staphylococcus aureus (S. aureus)* bacteria, regardless of the presence of silica. While the addition of silica slightly reduced the UV protection of coated fabrics, increasing the concentration of Pt to 1% increased the protection level to 45+. Various characterisation techniques including SEM, XPS, XRD, and TEM were employed to study the Pt-doping of TiO_2 nanoparticles, as well as the effect of Pt concentration, superhydrophilicity of silica, and the chemical composition of coatings on the functionalities of fabrics.

Keywords Doped-TiO_2 · Self-cleaning · Antibacterial fabrics · UV protection · Superhydrophilic coating

Supplementary Information The online version contains supplementary material available at https://doi.org/10.1007/s10570-024-06346-1.

E. Pakdel (✉) · X. Wang
School of Fashion and Textiles, Research Centre of Textiles for Future Fashion, The Hong Kong Polytechnic University, Kowloon, Hong Kong, China
e-mail: esfandiar.pakdel@polyu.edu.hk

X. Wang
e-mail: xungai.wang@polyu.edu.hk

W. A. Daoud
Department of Mechanical Engineering, City University of Hong Kong, Kowloon, Hong Kong, China

S. Kashi
Melbourne, Australia

M. Parvinzadeh Gashti
Department of Chemistry, Pittsburg State University, 1701 South Broadway Street, Pittsburg, KS 66762, USA

M. Parvinzadeh Gashti
National Institute for Materials Advancement, Pittsburg State University, Pittsburg, KS 66762, USA

Introduction

Research confirms that 39% of total greenhouse emissions in the textile industry is from product care measures by consumers such as washing, drying, and ironing (Tomšič et al. 2024; L. Zhang et al. 2023a, b). Household laundry of textiles produces a significant amount of wastewater containing detergents, microfibres, surfactants, and other pollutants, in addition to causing high energy consumption (Tomšič et al. 2024; L. Zhang et al. 2023a, b). Applying self-cleaning coatings on textiles can eliminate the need for frequent washing. The self-cleaning technology has been realised based on two mechanisms of i) the prevention of stain absorption on textiles through developing superhydrophobic and/or superoleophobic coatings (Pakdel et al. 2023), and ii) breaking down the absorbed stains using photocatalytic activity of semiconductors under a light source (Pakdel et al. 2020). The later strategy uses the synergistic effects of photocatalysis and superhydrophilicity to clean a stained surface (Wei et al. 2023). This functionality allows coated fabrics to degrade the pollutants under the irradiation of light, eliminating the contaminants such as stains, microorganisms, and even odours from their surface (Bai et al. 2022; Liu et al. 2023; Pakdel et al. 2017). Photocatalytic nanocoatings contain photoactive nanomaterials/microparticles such as titanium dioxide (TiO_2), and zinc oxide (ZnO) immobilised on substrates such as fibres through different approaches (Natsathaporn et al. 2023; Wang et al. 2023). These nanocoatings can be formed on textiles via methods such as dip-coating, layer-by-layer-assembly, sonication, in-situ synthesis, hydrothermal, and cross-linking to create self-cleaning coatings (Gashti et al. 2016; Wang et al. 2024; Zhao et al. 2017). Among different types of nanoparticles, TiO_2 stands out as an effective photocatalyst to impart novel photo-induced properties to textiles due to its cheap price, chemical stability, abundance, nontoxicity, and easy processing (Pakdel et al. 2014b; Wang et al. 2015). Although TiO_2 has several merits compared with other photocatalysts, there are certain deficiencies which have restricted its wide application. For instance, the lack of sensitivity to visible light due to its large band gap and relatively low photo-efficiency are two important drawbacks of TiO_2 (Bingham & Daoud 2011; Maqbool et al. 2024; Ni et al. 2007). To address these issues, several strategies such as doping TiO_2 with metal and non-metal elements, narrowing bandgap, blending TiO_2 with metal oxides, and dye sensitisation, have been used (Pakdel & Daoud 2013; Sun et al. 2020; Xie et al. 2020; Yu et al. 2016).

The photocatalytic mechanism of TiO_2 nanoparticles is triggered under the irradiation of light with energy equal or greater than its band gap, which is 3.2 eV and 3.0 eV for anatase and rutile crystalline forms, respectively (Pelaez et al. 2012). After the absorption of light energy, electrons are excited from the valence band (VB) to the conduction band (CB), producing pairs of negative electrons (e_{CB}^-) and positive holes (h_{VB}^+), which can initiate redox reactions on the surface of photocatalyst (Pelaez et al. 2012; Zhang et al. 2021). Electrons and holes react with oxygen and water molecules, producing superoxide anions $O_2^{\bullet -}$ and hydroxyl radicals ($^{\bullet}OH$) (Montazer & Pakdel 2011; Yu et al. 2016). These reactive species react with contaminants deposited on the surface of photocatalyst, breaking them down into harmless products such as CO_2 and H_2O (Pakdel et al. 2022; Zhai et al. 2022). Two key factors which can influence the overall photocatalytic efficiency are the band gap energy of TiO_2 and the recombination rate of electron–hole pairs, which are determined based on morphological and physical properties of the photocatalyst (Schneider & Curti 2023). Decreasing the band-gap energy and recombination rate of photogenerated electron–hole pairs can enhance harnessing the visible light, and overall photocatalytic activity (J. Zhang et al. 2023a, b). Research shows that doping TiO_2 with noble metals can shift its activation threshold towards the visible light region (Pakdel et al. 2022; Zhou et al. 2022). The efficiency of different types of noble metals such as Ag, Pt, Au, and Pd as dopants has already been confirmed (Feng et al. 2012; Yang et al. 2024). The efficiency of metal-doped photocatalysts depends on several parameters such as size, shape, morphology, interaction with the support material, synthesis method and chemical composition (Liu & Corma 2018; van Deelen et al. 2019). Of various noble metal dopants, the role of Pt in improving TiO_2's light absorption and delaying the decay of the photogenerated charge carriers has been reported (Feng et al. 2012; Gayle et al. 2022; Schneider et al. 2014). Platinised TiO_2-based photocatalysts have been widely used in different catalytic applications such as photocatalytic air purification, water splitting, and fuel production (Liu & Corma 2018;

Méndez et al. 2023; Vikrant et al. 2021). Modification of TiO_2 with Pt dopant can be classified into two strategies including metallisation of TiO_2, and doping of TiO_2 (Rosario & Pereira 2014). The former refers to the method by which metal nanoparticles are deposited on the surface of photocatalyst mainly via photodeposition. Under this condition, metals form Schottky barrier and act as a sink for the photogenerated electrons, reducing overall recombination. In the latter approach, which is based on doping, Pt ions are incorporated into the TiO_2 lattice substituting the Ti^{4+} ions. This process alters the bandgap and crystalline structure, changing TiO_2's response to visible light (Rosario & Pereira 2014). Comparing these two modification approaches, previous research confirmed that TiO_2 nanoparticles modified with ionic metal dopants possess a higher photocatalytic activity under visible light (Kim et al. 2005).

The effectiveness of noble metals such as Au and Ag as dopants in imparting enhanced functionalities to textiles has widely been reported (Abualnaja et al. 2021; Behzadnia et al. 2024; Milošević et al. 2023; Mollick et al. 2023; Pakdel et al. 2014a, 2014b, 2023; Tang et al. 2012). Concerning the functionality of metal-doped TiO_2 colloidal coatings on textiles, it was demonstrated that altering the synthesis procedure of TiO_2 colloids containing Au can result in varying photocatalytic activities (Pakdel et al. 2024a). The results showed that the Au-doped colloids synthesised via the photodeposition process exhibited weaker photocatalytic and antibacterial activities on the surface of cotton fabrics. The coated fabrics showed self-cleaning property under visible light generated by a solar simulator, and antibacterial activity against *E. coli* and *S. aureus* bacteria. Long et al. (Long et al. 2016) synthesised Pt-TiO_2 and N-TiO_2 and applied them on cotton fabrics using a dip-coating method. Monitoring the change in methyl orange dye concentration under visible light in the presence of fabrics coated with Pt-TiO_2 and N-TiO_2 showed 53.6% and 28.9% dye degradation, respectively, while pure TiO_2 caused only 19.2% degradation. The fabric coated with TiO_2/Pt discoloured the absorbed coffee stain within 20 h of irradiation under simulated sunlight. Montazer et al. (Montazer et al. 2012) reported that the TiO_2/Ag coatings synthesised via a photodeposition mechanism showed a photocatalytic self-cleaning effect on wool fabric under UVA and daylight irradiation. Similarly, the effectiveness of Ag, Au, and Pt dopants in enhancing the self-cleaning performance of wool and cotton fabrics has been reported (Pakdel et al. 2015a, 2014a, 2022). It was shown that using Ag and Au dopants led to moderate to severe colour changes on cotton fabrics, potentially affecting the applicability and aesthetic appeal of the products.

Among various metal dopants, limited research has been conducted on the effect of incorporating Pt into photocatalytic coatings for textile applications. Some key areas such as the impact of Pt doping on photo-induced self-cleaning, antibacterial activity, UV protection and washability of functionalised fabrics remain underexplored. Although Pt is an expensive dopant, it has widely been used to enhance the photocatalytic performance of TiO_2 nanoparticles. Pt-doped colloids effectively introduce novel functionalities to textiles without causing any colour changes, which is an advantage compared with other types of noble metal dopants. It has also been reported that Pt can be a more effective dopant compared with other commonly used alternatives such as Ag for boosting the photoactivity of TiO_2 nanoparticles (Bumajdad & Madkour 2014). The synergistic effects of Pt doping and superhydrophilic silica on enhancing novel functionalities on textiles have not yet been fully explored. Therefore, it is worthwhile to thoroughly investigate how Pt and silica can synergistically influence on the functionalities of superhydrophilic titania-based coatings on cotton fabrics, elucidating their role in achieving self-cleaning, antibacterial activity, and UV protection on textiles. Moreover, the modification of TiO_2 with ionic Pt dopant has not been reported for textile applications and its effects on chemical and physical characteristics of cotton fabrics are unknown. Therefore, in this study, colloids of TiO_2/Pt/SiO_2 colloids were synthesised through the low temperature sol–gel method and applied to cotton fabrics via a dip-pad-dry-cure method. Different properties of fabrics such as self-cleaning, photocatalytic activity under UV and visible light, MB dye degradation kinetics, antibacterial activity against *E. coli* and *S. aureus* bacteria, UV protection, mechanical properties, and washing fastness of applied coatings were thoroughly investigated and the role of each individual ingredient was clarified.

Experimental

Materials and chemicals

A woven cotton fabric with the mass of 135 g/m^2 was used as the substrate. Titanium tetra isopropoxide (TTIP) 97% and tetra ethyl orthosilicate (TEOS) 98% were purchased from Sigma-Aldrich and used as the precursors of TiO_2 and SiO_2 sols, respectively. Chloroplatinic acid hexahydrate ($H_2Cl_6Pt \cdot 6H_2O$) (Sigma-Aldrich) was utilised as the precursor of Pt.

Synthesis of colloids

TiO_2 sol was prepared through hydrolysis and condensation reactions of TTIP in an aqueous solution in the presence of acetic acid. Nitric acid (HNO_3) was added into the mixture of TTIP, distilled water and acetic acid, then the mixture was stirred at 60 °C for 2 h obtaining a transparent TiO_2 colloid. To synthesise the TiO_2/Pt colloids, predetermined amount of metal precursor was added to the mixture and was refluxed at 60 °C for 2 h resulting in transparent sols. Four Pt:Ti molar ratios including 0.01%, 0.1%, 0.5% and 1% were used to synthesise the colloids. The silica sol was prepared from TEOS in an acidic condition (pH = 3) after 2 h of stirring at room temperature. The silica sol was added to the TiO_2 and TiO_2/Metal colloids based on the molar ratios of TiO_2/SiO_2 30/70 and 50/50. After stirring at room temperature for 1 h, the ternary nanocomposite sols were obtained. In total, 13 different colloids were synthesised as listed in Table 1. For simplicity of naming ternary $TiO_2/Pt/SiO_2$ colloids, only the ratio of ingredients was used to label them in the text.

Fabric surface coating

Cotton samples were scoured in a water bath containing 2 g/L nonionic detergent (Kieralon F-OL-B) at 40 °C for 20 min. After a rinse with running deionised water, the cotton samples were dried at room temperature for 24 h. The coating process was carried out based on the dip-pad-dry-cure process. The scoured fabrics were immersed into the sols for 1 min and then the additional uptake was removed during the padding step using an automatic padding machine with the rotating speed of 7.5 rpm and 2.75 kg cm^{-2} pressure. The fabrics were then neutralised with the fume of ammonia hydroxide 25%. The coating process was completed by drying the samples at 80 °C for 5 min and then curing at 120 °C for 5 min.

Testing self-cleaning and wet photocatalytic property

The photocatalytic self-cleaning test was conducted under UV and visible light sources produced by nine BLB bulbs of Philips TL-D 18 W with a maximum intensity at wavelength (λ) 370 nm and fluorescent lamps of Philips 30 W, respectively, positioned 40 cm above the samples. The fabrics were stained with concentrated coffee solution and exposed to light sources up to 8 h.

To analyse the wet photocatalytic activity of fabrics, 1 g of fabrics was cut into 1 × 1 cm pieces and then added to 50 ml of 10 mg/L MB solution (pH = 1). Fabrics were stirred in the dark for 30 min to achieve adsorption–desorption equilibrium prior to light irradiation on samples. UV and visible light irradiations were generated by five Philips UVA and fluorescent lamps, respectively positioned at 10 cm above the samples. The degradation of MB was assessed based on measuring the variation of peak intensity at 664 nm

Table 1 The list of colloids synthesised through the sol–gel method and applied to fabrics

Number	Colloid name	Number	Colloid name
1	TiO_2	8	$TiO_2/Pt/SiO_2$ 50/0.5/50
2	TiO_2/Pt 0.01%	9	$TiO_2/Pt/SiO_2$ 50/1/50
3	TiO_2/Pt 0.1%	10	$TiO_2/Pt/SiO_2$ 30/0.01/70
4	TiO_2/Pt 0.5%	11	$TiO_2/Pt/SiO_2$ 30/0.1/70
5	TiO_2/Pt 1%	12	$TiO_2/Pt/SiO_2$ 30/0.5/70
6	$TiO_2/Pt/SiO_2$ 50/0.01/50	13	$TiO_2/Pt/SiO_2$ 30/1/70
7	$TiO_2/Pt/SiO_2$ 50/0.1/50		

wavelength at different irradiation intervals measured by UV–vis spectrophotometer (Varian-carry 300).

The MB dye degradation kinetics were analysed based on pseudo-first order and pseudo-second-order kinetic models using Eq. 1 (Eq. 1) and Eq. 2, respectively. C_t was the MB dye concentration at time (t) and C_0 was the initial concentration of dye. K_1 and K_2 were the reaction rate constants based on pseudo-first-order and pseudo-second-order kinetics, respectively.

$$-\ln\left(C_t/C_0\right) = k_1 t \tag{1}$$

$$1/C_t = 1/C_0 + k_2 t \tag{2}$$

The MB dye degradation percentage in the presence of fabrics was calculated using Eq. 3.

$$\text{Dye degradation}\ (\%) = \left[\left(C_0 - C_t\right)/C_0\right] \times 100 \tag{3}$$

Measuring the UV protection property

UV protection of fabrics was measured using a spectrophotometer (UPF and UV Penetration/Projection Measurement System, Model: YG902, China). The values of UPF, and transmitted ray were automatically calculated by the instrument. Eight spots of each sample were tested, and the average values were reported.

Washing fastness test

The washing fastness test was carried out using a launder-ometer (FONG'S, Hong Kong) based on the AATCC 61–2010 standard test method. Each sample was washed for 10 times in a bath containing detergent and the durability of samples were tested based on the variation of UPF level of fabrics. To this end, fabrics were cut into 10×5 cm pieces and put in separate canisters containing 200 ml water, 1.85 g/L detergent, and 10 steel balls. Each wash cycle was carried out at 40 °C for 45 min, followed by drying at 50 °C for 1 h in an over. The washed samples were conditioned in laboratory (20 ± °C and 65 ± 2% relative humidity) overnight.

Assessment of Antibacterial activity:

Gram-negative *Escherichia coli (E. coli)* and Gram-positive *Staphylococcus aureus (S. aureus)* bacteria were used as testing microorganisms to assess the antibacterial activity of fabrics according to the AATCC 100–2004 test method (Pakdel et al. 2024b). Prior to the test, the samples were sterilised with UV ray for 45 min. The bacteria suspension with 1×10^5 colony forming units (cfu)/ml was prepared by adding microorganisms to tryptic soy broth. Each fabric was cut circular with the diameter 48 mm, and inserted into sterile gamma container, and then 1 ml of bacteria inoculum was added into the container, followed by incubation at 37 °C for 24 h. Next, 100 ml of saline was added to each container followed by shaking, and then 1 ml of the prepared solution was cultured in petri-dishes containing tryptic soy agar medium. The petri-dishes were incubated at 37 °C for 24 h and then the growth rate of bacteria colonies in each agar plate was observed and their photographs were recorded.

Testing mechanical properties of fabrics

The tensile strength test of fabrics was conducted using Instron 30 kN Tensile Tester instrument (USA). The tensile strip test was performed according to the standard test method of ASTM D5035-11 in both warp and weft directions. The specimens were mounted to the clamps of instrument and the test was conducted based on the constant rate of extension (CRE) with the elongation speed of 300 ± 10 mm/min and the gauge length of 75 mm. Three specimens in each direction were tested and the average values were reported.

The bending rigidity of coated fabrics was measured based on the AS 2001.2.9 standard test method using a fixed-angle fabric stiffness tester (SDL ATLAS). All the mechanical tests were carried out for both weft and warp directions of fabrics. This test was repeated at least three times for three specimens from each sample, and the average results were reported. The stiffness of fabrics was compared based on the bending modulus (q) of fabrics in N/m^2 (Eqs. 4 and 5).

$$G\,(uN.m) = m \times C^3 \times 9.807 \times 10^{-6} \tag{4}$$

$$q\,(N/m) = \left(12 \times G \times 10^3\right)/t^3 \tag{5}$$

where G was the flexural rigidity of fabrics, C was the bending length (mm) of the tested specimen, m was the fabric mass per unit area (g/m^2), and t was the thickness of fabrics (mm).

Measuring the air permeability of fabrics was carried out using a textile air permeability tester (TEXTEST AG, FX3300-III, Switzerland) according to the standard test method of BS 5636 (Great Britain). All samples were pre-conditioned in the laboratory for 12 h prior to the tests.

Characterisation instruments

The surface morphology of fibres was investigated using scanning electron microscopy (SEM) images captured using KYKY-EM3200 (China). The morphology of washed sample was further characterised using Zeiss Supra 55VP instrument. Transmission electron microscopy (TEM) images of nanoparticles were taken using JEOL JEM-2100F with an accelerating voltage of 200 kV. Selected area electron diffraction (SAED) patterns were taken using the same TEM instrument. Chemical composition of applied coatings was examined using the X-ray photoelectron spectroscopy technique (Thermo Fisher Scientific Nexsa). The crystallinity of fabrics was tested using X-ray diffractometer (X'Pert Powder, PANalytical, Netherlands) with a Cu Kα radiation over 2θ range of 15–50° operating at 40 kV and 30 mA. Fourier transform infrared (FTIR) analysis was performed using Varian 1000 instrument equipped with an attenuated total reflectance (ATR) accessory. The UV–Vis spectra were obtained using UV–vis spectrophotometer (Varian-carry 300). The light reflectance of fabrics was tested using a Carry 5000 UV–vis–NIR spectrophotometer equipped with a diffuse reflectance accessory over a 200–800 nm wavelength range.

Results and discussion

In this work, pure and modified TiO_2 colloids were synthesised through the sol–gel method and applied to cotton fabrics to achieve novel functionalities as shown in Fig. 1 of fabrics.

Optical properties of colloids

Figure 2a shows that through incorporating Pt into the sol–gel synthesis of TiO_2, the bluish colour of pure TiO_2 changed to a pale yellow, which was intensified by increasing the concentration of Pt. Based on the obtained UV–vis spectra (Fig. 2b and c), increasing the concentration of Pt in the colloids, led to a higher visible light absorption, which was related to the excitation of electrons from the dopant ions to the conduction band of TiO_2 (Choi et al. 2010; Nishiyama et al. 2015). Also, this shift of light absorption to visible region can be related to forming the impurity levels of Pt^{4+} in the TiO_2 lattice, the generation of oxygen vacancy induced by the doped ions, and the formation of PtO species on the surface of TiO_2 (Choi et al. 2010; Hu et al. 2015). Additionally, adding silica further enhanced the visible light absorption of colloids (Fig. 2d), which is in good agreement with previous findings (Pakdel et al. 2024a). The deposition of TiO_2-based nanocomposites on the surface of fabrics, reduced the UV reflectance of fabrics over the UV region, which was due to the intrinsic UV absorption behaviour of TiO_2 nanoparticles (Fig. 2e). This implied a better UV protection property of coated fabrics compared with pristine cotton. The existence of silica and Pt on the surface of fabrics did not show a tangible impact on the optical properties of fabrics over visible light region (400–700 nm) as can be seen in Fig. 2e.

Surface characterisation of fibres

The SEM images confirmed the formation of a thin coating layer on fibres without any severe aggregation of nanoparticles (Fig. 3). Incorporation of Pt precursor into the colloid resulted in a rougher surface, but the developed coatings were still uniform. Silica-containing coatings were even and uniform, without any obvious aggregations. The applied coatings deposited on the surface of fibres, and they did not lead to the full blockage of the pores among fibres. Figure 3b illustrates the TEM images of TiO_2 and TiO_2/Pt nanoparticles synthesised through the sol–gel method (Fig. 3b). The parallel arrays of TiO_2 lattices showed the interlayer distances of 0.348 nm (Fig. 3b and d) with the lattice strips appearing more sequential than those of Pt-doped TiO_2, implying that the Pt ions were successfully doped into the crystallite (Hu et al. 2015). The analysis of TiO_2's SAED pattern showed the (101), (004), (200), (204), and (211) planes which is in good agreement with literature (Pakdel et al. 2018). The slight expansion of TiO_2 lattice spacing

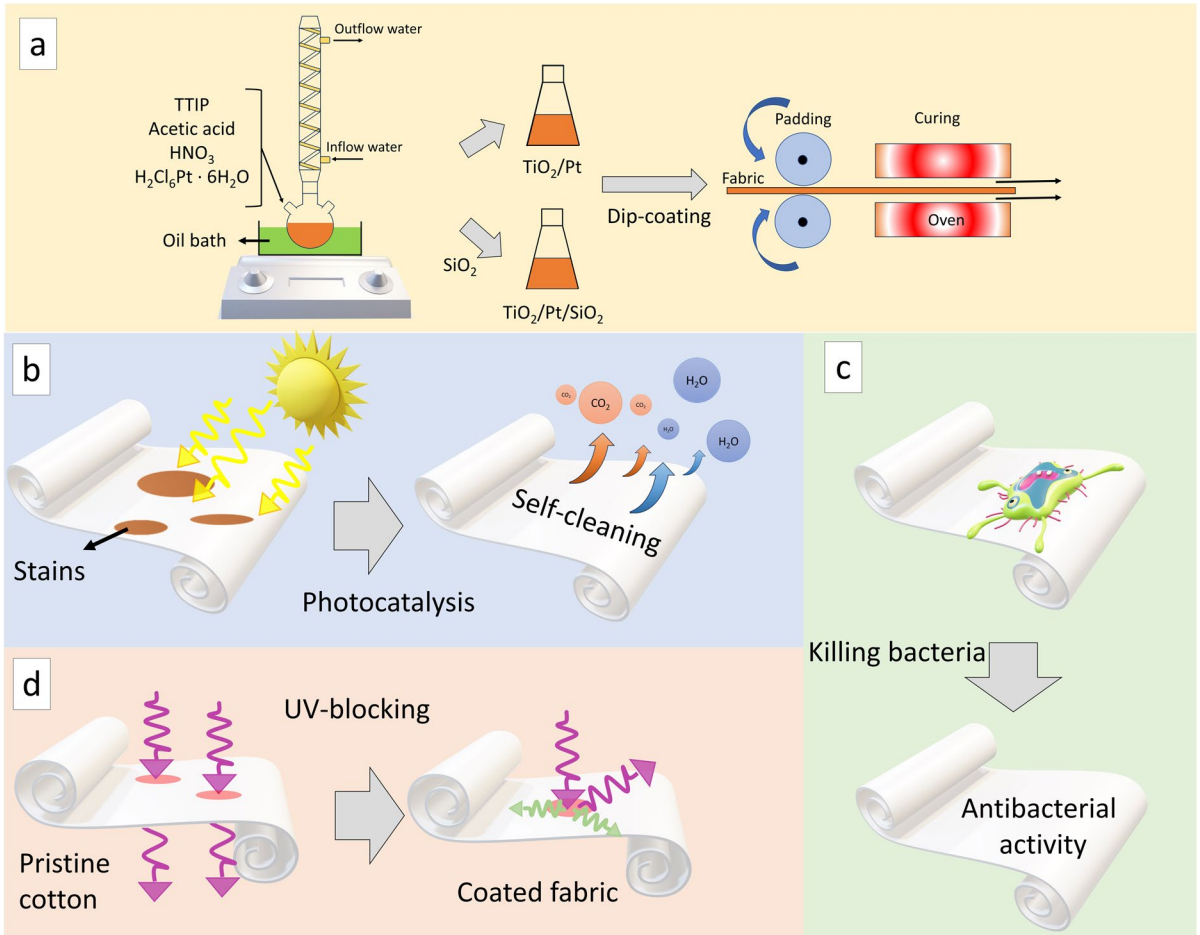

Fig. 1 (**a**) Schematic illustration of the sol–gel synthesis of TiO_2/Pt and TiO_2/Pt/SiO_2 colloids and the coating process on fabrics, (**b**) photocatalytic self-cleaning fabrics, (**c**) antibacterial activity developed on fabrics, d) UV protection mechanism on coated fabrics

after doping can be due to the incorporation of Pt ions in TiO_2 lattice, which in turn distorted the crystalline dimensions of anatase (Hu et al. 2015; Zang et al. 2024).

The chemical composition and state of elements in the developed coatings were examined using XPS analysis (Fig. 4). On the fabric coated with pure TiO_2, the peaks related to O1s, C1s and Ti 2p were detected confirming the deposition of a titania layer at the outer surface of fibres. The Ti $2p_{3/2}$ and Ti $2p_{1/2}$ peaks appeared at binding energies of 457.3 eV and 463 eV with 5.7 eV apart, confirming the presence of Ti^{4+} in the crystal (Xue et al. 2020). It was also noticed that the synthesised TiO_2 contained a small concentration of Ti^{3+} according to the weak peak appeared at 458 eV (Fig. 4a). After doping with Pt, the peak intensity of Ti $2p_{3/2}$ related to Ti^{4+} decreased, and the Ti^{3+} peak increased, indicating the removal of oxygen from the lattice (Fig. 4b) (Bharti et al. 2016). The presence of Ti^{3+} can influence the electron–hole pairs recombination mainly by forming oxygen vacancies in the band gap and thereby contributing to the enhanced visible-light activity of TiO_2 (Mohajernia et al. 2020). In the Pt-doped TiO_2 photocatalyst (Fig. 4b), two main peaks of Pt 4f 7/2 and Pt 4f 5/2 were deconvoluted into four smaller peaks. The larger deconvoluted peaks at 72.3 eV and 75.3 eV are assigned to PtO existed on the photocatalyst, and the weaker peaks at 73.8, and 76.3 eV correspond to PtO_2, which is in good agreement with Hu et al. (Hu et al. 2015; Kim et al. 2005; Wu et al. 2011). Comparing the ionic radius of Pt^{4+} (0.765 Å),

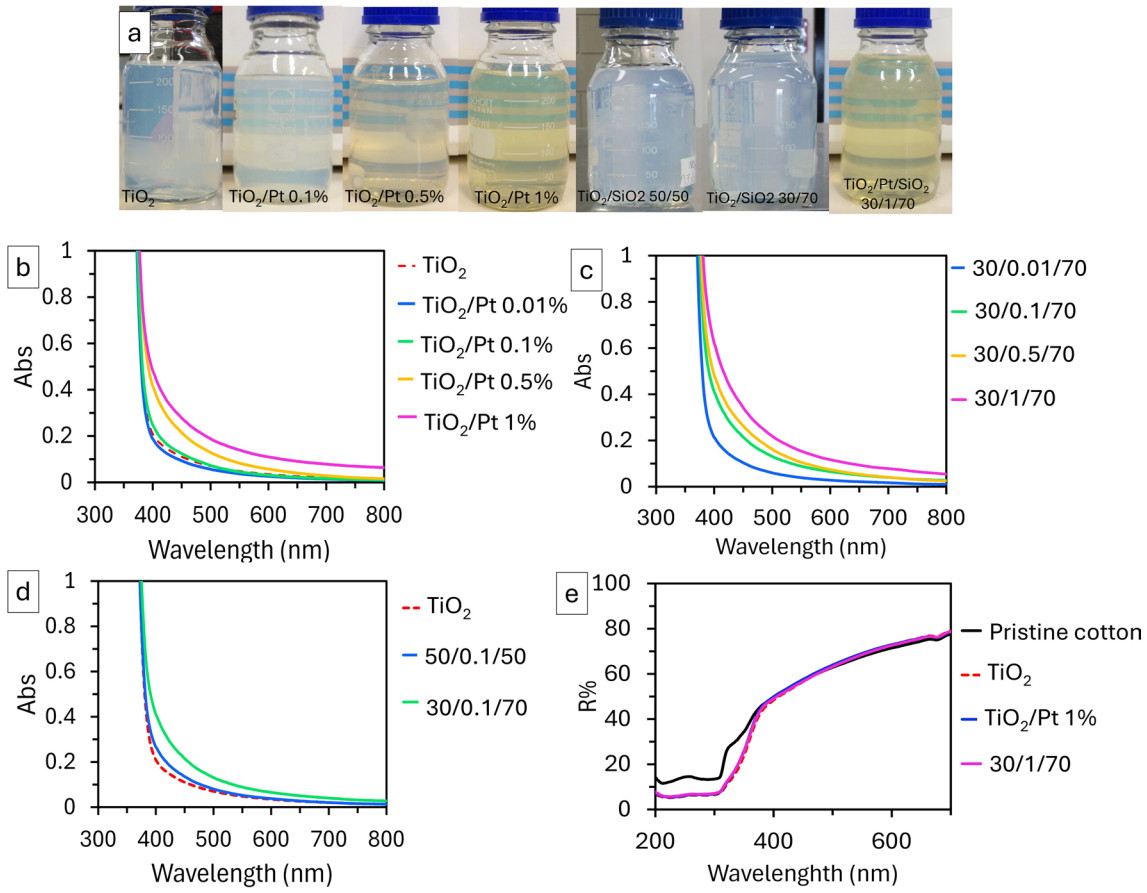

Fig. 2 (**a**) Photographs of some of the colloids synthesised through the sol–gel method; UV–vis spectra of (**b**) TiO_2/Pt colloids, and (**c**) TiO_2/Pt/SiO_2 colloids; (**d**) UV–vis spectra showing the effect of silica on the light absorption of colloids; (**e**) UV–Vis diffuse reflectance of cotton fabrics

Ti^{4+} (0.745 Å) and Pt^{2+} (0.94 Å), it can be concluded that Pt^{4+} ions can substitute Ti^{4+} ions due to their similar ionic radii, thereby doping the TiO_2 lattice (Hu et al. 2015; Kim et al. 2005; Zang et al. 2024). It has been reported that the Pt^{2+} peaks can appear because of the existence of PtO and $PtCl_2$ on the surface of photocatalysts (Hu et al. 2015). However, no Cl peak was detected in the corresponding spectrum, indicating that the Pt^{2+} peaks on the tested sample are attributed to PtO formed on the surface of TiO_2. The Pt-related peaks weakened after adding silica, due to the silica's effect on masking the elements and changing the surface chemical composition. As for pure TiO_2, O1s peaks can be fitted with three peaks positioned at binding energies of 529 eV, 530.2 eV, and 531.2 eV, corresponding to the lattice oxygen bound to Ti^{4+}, absorbed hydroxyl groups, and the presence of OH terminal groups whose oxygen coordinated with Ti^{4+} ion, respectively (Bharti et al. 2020). Doping TiO_2 with Pt led to weaker O 1 s and Ti 2p peaks intensity which can be due to the formation of Pt layer on TiO_2, altering the amount of lattice oxygen, and having a less amount of OH groups on the surface of coating. Adding silica further changed the O1s peak shape and intensity, where its addition decreased and increased peak intensities at 529 eV, and 531.2 eV, respectively. The former can be due to the coverage of TiO_2 nanoparticles and therefore having a less amount of lattice oxygen accessible to XPS. The latter can be linked to the role of silica in developing superhydrophilicity on fabrics and providing more hydroxyl groups due to introducing Si–OH and adsorbed water molecules on the surface (Bai et al. 2022; Krishnan et al. 2017). The sharp Si 2p peak can be deconvoluted into three

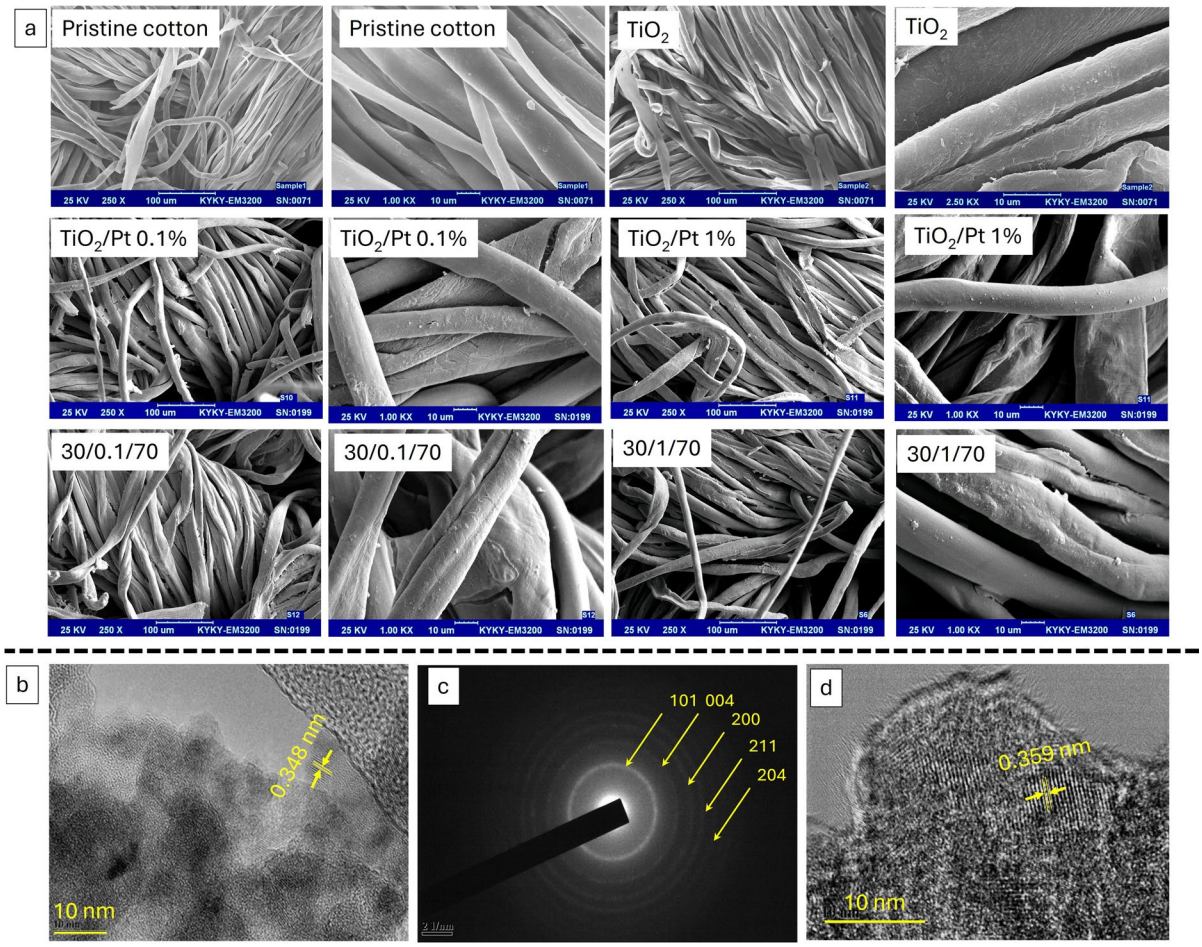

Fig. 3 SEM images of cotton samples coated with TiO_2, TiO_2/Pt and TiO_2/Pt/SiO_2 colloids (magnifications: × 250 and × 2500); (**b** and **c**) TEM image and SAED pattern of TiO_2, and (**d**) TEM image of TiO_2/Pt/SiO_2 1% nanocomposite

main peaks at around 100.7 eV, 102 eV, and 103 eV, corresponding to Si–C, Si–OH and Si–O–Si, respectively (Post et al. 2018).

XRD patterns of pristine and coated fabrics showed characteristic peaks related to cellulose crystalline structure and anatase TiO_2 (Fig. 5a). The main sharp peak at $2\theta = 22.7°$ was because of the crystalline structure of cellulose, and its intensity decreased after applying coatings. On coated fabrics, the small shoulder peak at $2\theta = 25.4°$ was due to the anatase crystalline structure of TiO_2 deposited on cotton fibres. No diffraction peaks were observed for Pt, indicating that the metal ions were dispersed in the lattice of TiO_2 (Choi et al. 2010; Nishiyama et al. 2015). FTIR spectra of samples showed the characteristics peaks of cellulose (Fig. 5b). The broad peaks at 3330 cm^{-1} and 3280 cm^{-1} were related to intra-molecular hydrogen bonding and inter-molecular hydrogen bonding of cellulose, respectively (Abidi et al. 2014). The peaks located at 1100 cm^{-1}, 1053 cm^{-1} and 1018 cm^{-1} were assigned to the anti-symmetric C–O–C stretching vibration, C–O stretching mode, and C–O stretch of cellulose, respectively (Abidi et al. 2014). The small shoulder peak at 1140 cm^{-1} was from C–O–C stretching within cellulose. This peak can also be related to the asymmetric stretching of Si–O–Si on the fabric coated with colloidal solution (Abidi et al. 2007). The peaks at 1240 cm^{-1} and 1400 cm^{-1} were from in-plane bending of C–O–H, which have been reported as fingerprints of secondary wall in cotton structure (Abidi et al. 2008). These peaks remained almost unchanged after coating process. The small peak at

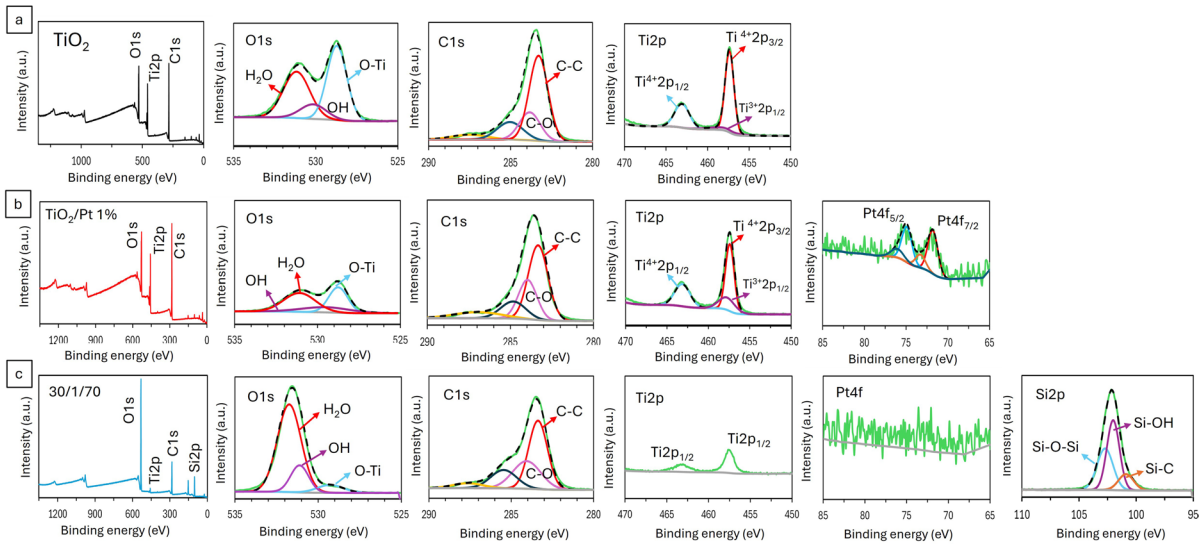

Fig. 4 XPS analysis of fabrics coated with (**a**) TiO_2, (**b**) TiO_2/Pt 1%, and (**c**) 30/1/70 colloids, (The dashed line represents the simulated graph based on the deconvoluted curves)

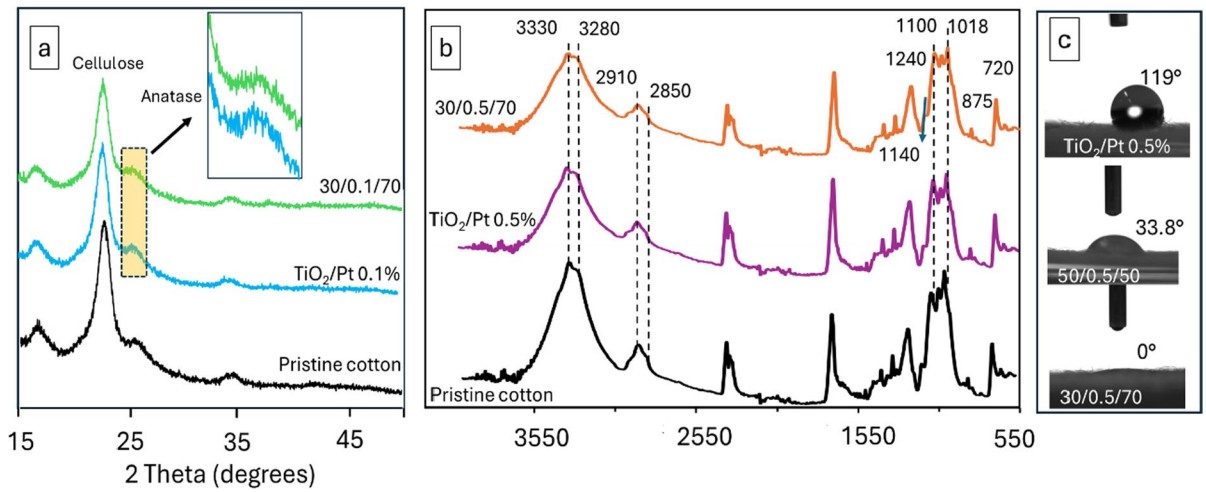

Fig. 5 (**a**) XRD patterns of pristine cotton and representative fabrics coated with Pt-modified colloids; (**b**) FTIR spectra of pristine and coated cotton fabrics; (**c**) the effect of silica on reducing the WCA of coated fabrics

875 cm^{-1} was associated with the β-linkage of cellulose (Abidi & Manike 2018). The peak at 1635 cm^{-1} was due to the adsorbed water in the amorphous parts of cellulose, via hydrogen bonding. Its amount decreased in treated fabrics indicating the interactions of applied coatings with amorphous regions of cellulose. The peak at 720 cm^{-1} was assigned to CH_2 rocking in crystalline cellulose and its intensity remained unchanged after coating process. The peaks at the region of 2910 cm^{-1} to 2850 cm^{-1} originated from CH_2 asymmetrical and symmetrical stretching, respectively (Abidi et al. 2014). Previous publications assumed that these peaks were from non-cellulosic substances which may explain their weaker intensity after treatment with acidic colloids (Abidi et al. 2014). The peaks related to TiO_2 and SiO_2 were mostly overlapped with the peaks of cotton. For example, the peaks related to asymmetric and symmetric stretching

vibrations of Si–O–Si can appear at 650 cm^{-1}, and 780 cm^{-1}, respectively, overlapping with the cotton-related peaks. The peaks related to Ti–O–Si stretching appear around 950–1000 cm^{-1} which have been overlapped with the C–O–C and C–O bands of cellulose (Pakdel et al. 2018). Analysing the WCA of fabrics showed that the fabric coated with TiO_2/Pt colloid was hydrophobic with a contact angle 119°. Adding silica with the ratios of TiO_2/SiO_2 50/50 and 30/70 rendered the fabrics hydrophilic and superhydrophilic, respectively (Fig. 5c). The higher hydrophilicity of fabrics in the presence of silica is in good agreement with the XPS findings.

Photocatalytic self-cleaning property

Testing the photocatalytic self-cleaning of coated fabrics showed that the sample coated with pure TiO_2 did not remove the coffee stains neither under UV nor visible light even after 8 h of irradiation (Fig. S1). After doping TiO_2 with Pt, the fabrics showed a weak self-cleaning under both types of light sources, failing to completely decompose the stains. However, it was observed that after adding silica, the self-cleaning property significantly improved under both UV and visible light. Increasing the concentration of silica from TiO_2/SiO_2 50/50 to 30/70 ratio, led to a stronger photocatalytic self-cleaning on platinised cotton fabrics (Figs. 6 and 7).

Wet photocatalytic activity

Given the better self-cleaning property of coatings developed based on TiO_2/Pt/SiO_2 30/Pt/70 ratios, their photocatalytic activity was further assessed quantitatively. The analysis of the photocatalytic efficiency was conducted by monitoring the degradation rate of MB in the presence of coated fabrics under both UV and visible light (Fig. 8 and 9). It was noticed that the fabrics showed different tendencies in absorption of MB dye during the initial absorption–desorption process in dark. In the presence of silica, the dye adsorption significantly increased, while Pt addition and its concentration had negligible effects. In the binary TiO_2/Pt colloids, the concentration of Pt influenced on the photocatalytic activity of coatings under both types of light sources. For instance, TiO_2/Pt 0.1% led to a weaker photocatalytic performance compared to pure TiO_2, and after increasing the concentration of Pt dopant to 1%, the photocatalytic performance increased under visible light. The major dye removal was achieved after adding superhydrophilic silica to the coating formulations. For instance, the

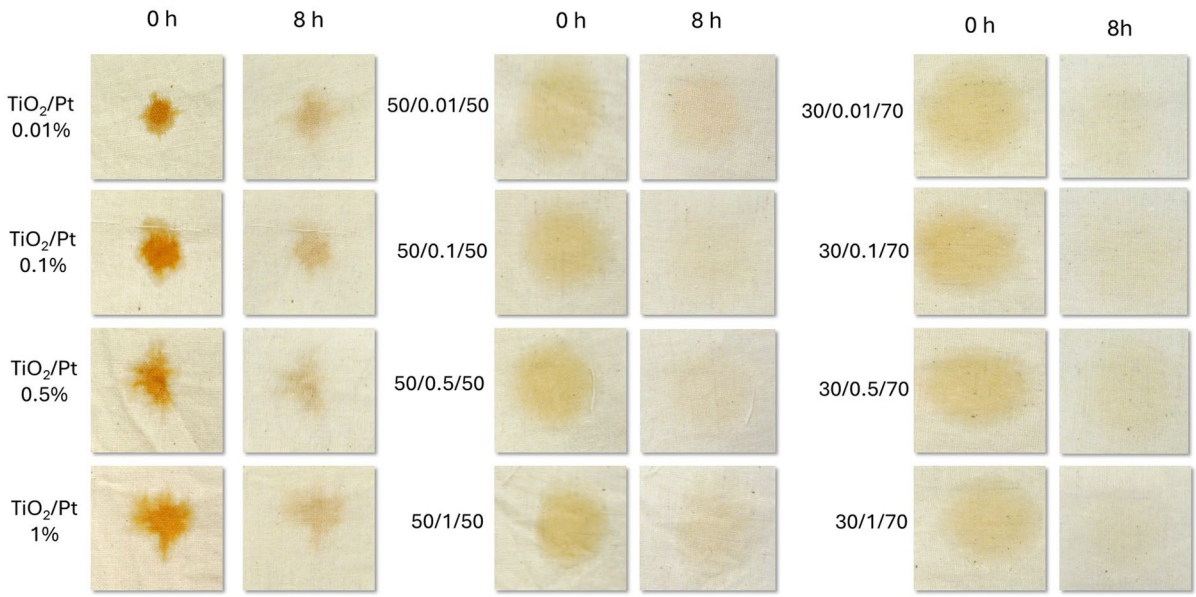

Fig. 6 Self-cleaning property of fabrics under UV

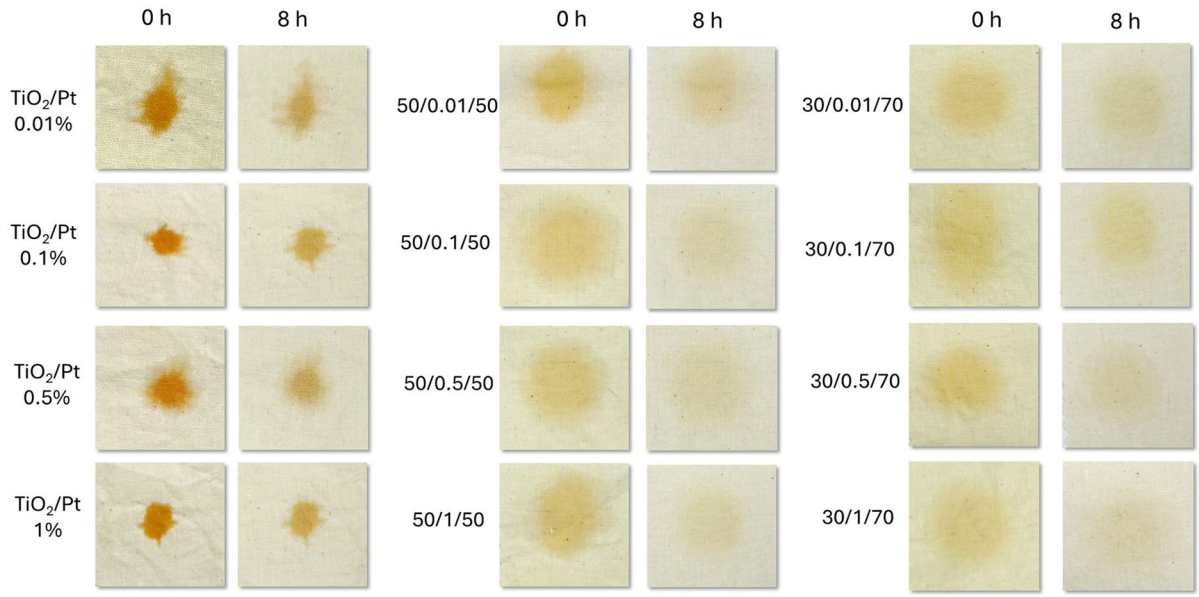

Fig. 7 Self-cleaning property of fabrics under visible light irradiation

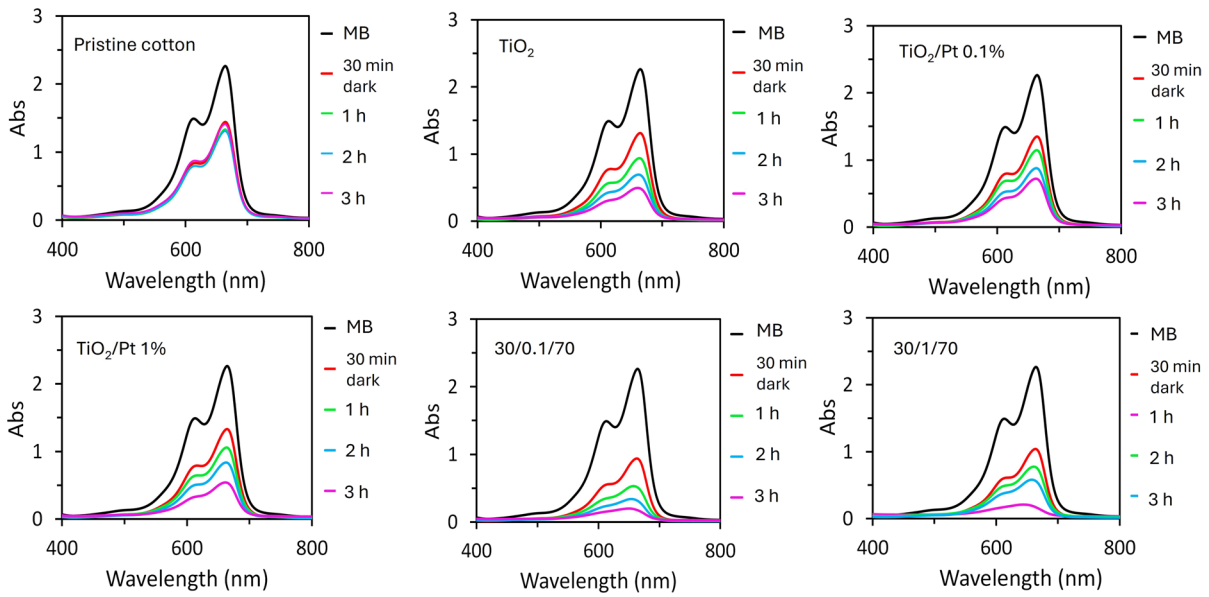

Fig. 8 Photocatalytic degradation of MB dye under UV in the presence of cotton fabrics

fabric coated with 30/1/70 colloid exhibited 43.5% and 39% higher MB degradation efficiency after 3 h of irradiation under visible light compared to the samples coated with pure TiO_2 and TiO_2/Pt 1%, respectively (Table 2).

MB dye degradation kinetics

The degradation kinetics of MB in the presence of fabrics under UV and visible light irradiation was further analysed based on the pseudo-first order and pseudo-second-order kinetic models (Fig. 10). As a

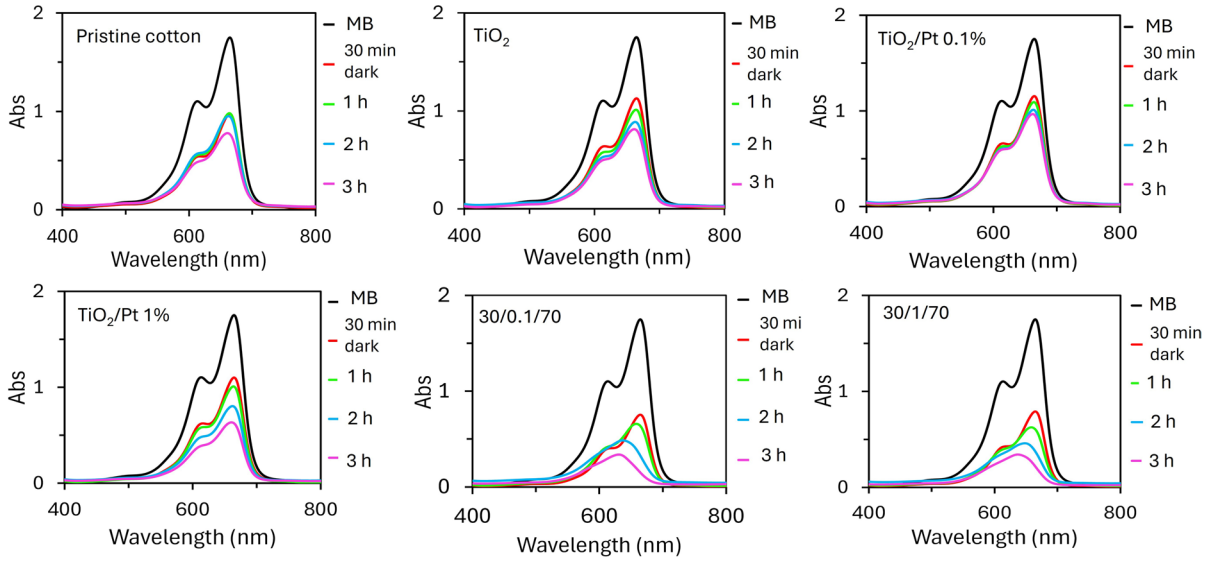

Fig. 9 Visible-light-induced photocatalytic degradation of MB in the presence of fabrics

general trend, it was observed that the degradation of MB in the presence of coated fabrics was faster under UV irradiation compared to visible light, regardless of the coating formulation. The concentration of Pt and the presence of silica both had significant impacts on the overall reaction rates and the pace of reactions (Table 3). Among different coatings, the 30/1/70 formulation showed superior photocatalytic activity under both UV and visible light. In general, for ternary colloidal coatings on cotton fabrics, the second-order kinetic model provided a better fit for the MB degradation process, according to the calculated correlation coefficients (R^2). The 30/1/70 coating provided the highest rate constants for both first and second-order-kinetic models. For this type of photocatalytic coating, the calculated K_1 and K_2 constant values were 0.539 h^{-1} and 0.128 L/g.h under UV irradiation, and 0.363 h^{-1} and 0.073 L/g.h under visible light, respectively.

Proposed photocatalytic mechanisms

Based on the obtained results, the effect of Pt dopant and silica on photocatalytic property of fabrics can be proposed. It was observed that the fabric coated with 30/1/70 formulation showed higher MB and coffee stain removal under UV and visible light. There are several reasons behind this improvement, including i) the incorporation of Pt^{4+} ions into the lattice of TiO_2 and the formation of a new impurity level, ii) the deposition of PtO on the surface of photocatalyst, and iii) the creation of Ti^{3+} defects in the doped photocatalyst. As one of the contributing factors, the improved visible-light-induced photocatalytic activity of the TiO_2/Pt 1%-coated fabric was related to the incorporation of Pt^{4+} ions into the lattice of TiO_2, as confirmed by the XPS analysis. Therefore, it is plausible to say that under the irradiation of visible light, the light energy can excite electrons from

Table 2 Adsorption, and photocatalytic degradation of MB dye by fabrics

Samples	Pristine cotton	TiO_2	TiO_2/Pt 0.1%	TiO_2/Pt 1%	30/0.1/70	30/1/70
MB dark uptake (%)	33	37	35.5	37	56.5	53.2
MB degradation under UV (%)	34.11	78.27	66.64	70.52	86.94	88.17
MB degradation under visible light (%)	46.3	55.15	43.72	56.98	75.79	79.15

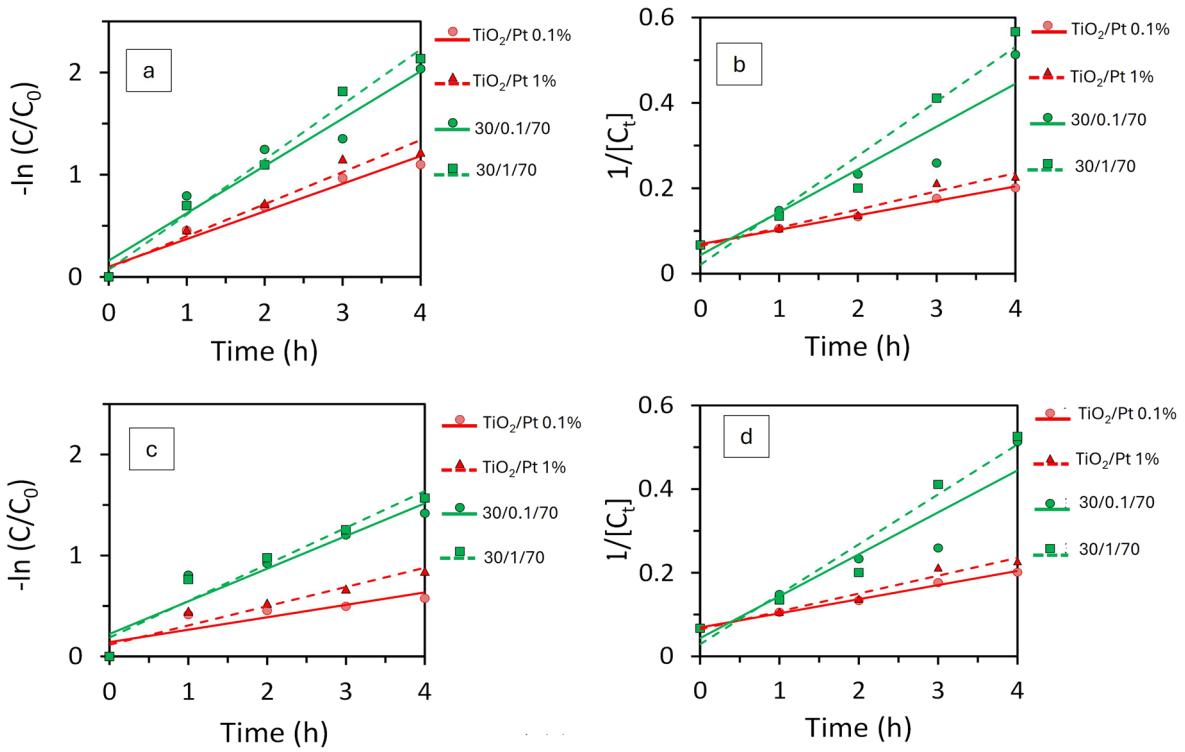

Fig. 10 MB degradation kinetics under irradiation in the presence of fabrics, a) pseudo-first-order kinetic under UV, b) pseudo-second-order kinetic under UV, c) pseudo-first-order kinetic under visible light, d) pseudo-second-order kinetic under visible light

Table 3 Kinetics of MB dye degradation by fabrics coated with Pt-doped colloids under UV and visible light irradiation

Samples	UV				Visible light			
	1st order	2nd order			1st order		2nd order	
	K_1 (h^{-1})	R^2	K_2 (L/g.h)	R^2	K_1 (h^{-1})	R^2	K_2 (L/g.h)	R^2
TiO_2/Pt 0.1%	0.271	0.962	0.034	0.994	0.123	0.752	0.014	0.805
TiO_2/Pt 1%	0.314	0.960	0.042	0.967	0.191	0.910	0.025	0.958
30/0.1/70	0.463	0.947	0.100	0.888	0.323	0.890	0.060	0.971
30/1/70	0.539	0.986	0.128	0.946	0.363	0.936	0.073	0.981

the impurity level of $Pt^{4+}$to the conduction band of TiO_2 (Hu et al. 2015). The remained holes at the Pt^{4+} impurity level migrate to the valence band of deposited PtO, reducing the recombination of electron–hole pairs (Hu et al. 2015; Ren et al. 2017). In addition, the presence of PtO on the outer surface of the platinised photocatalysts can contribute to the improved photocatalytic activity. It has been reported that PtO can be excited under visible light and inject electrons into the conduction band of TiO_2, extending the photoefficiency of the modified TiO_2 to visible light (Hu et al. 2015). The third proposed contributing mechanism is the formation of self-doping Ti^{3+} defects in the modified photocatalysts (Xiu et al. 2020). Ti^{3+} defects can form intermediate gap between the valence band and conduction band of TiO_2, promoting the visible light absorption and separation of photogenerated electron–hole pairs (Xiu et al. 2020). Therefore, the combining effects of all these mechanisms can contribute to reducing the overall recombination rate of photogenerated electrons-holes and enhancing

the photocatalytic activity of TiO_2 nanoparticles. Another key parameter which should be considered is the presence of silica in the vicinity of the doped photocatalyst. The increased photocatalytic activity in the presence of silica was also attributed to the enhanced superhydrophilicity of the fabrics, and the role of extra water molecules which exist on the coated surface (Drelich et al. 2011). This feature boosted the photocatalytic reactions and production of reactive species such as hydroxyl radicals under irradiation (Bai et al. 2022; Pakdel & Daoud 2013). The addition of silica can i) prevent the agglomeration of TiO_2 nanoparticles on the coated surface, ii) boost the surface acidity on the photocatalyst by creating Bronsted acidic sites due to the formation of Ti–O-Si bonds (Wolek et al. 2023), and iii) increase the overall surface area depending on its concentration and synthesis approach (Pakdel et al. 2018; Romero-Morán et al. 2021). Figure 11 proposes the main Pt-related mechanisms in photocatalytic activity of a superhydrophilic TiO_2/Pt/SiO_2 coating under UV and visible light.

Antibacterial activity of fabrics

Figure 12 confirmed that the addition of Pt introduced an effective antibacterial activity against both *E. coli* and *S. aureus* bacteria as gram negative and positive microorganisms to fabrics. The obtained results showed that pure TiO_2 and TiO_2/SiO_2 30/70 coatings did not show any antibacterial activity on cotton fabric which can be related to the absence of light to activate their photocatalytic activity (Fig. S2) (Natsathaporn et al. 2023; Pakdel et al. 2024a). Increasing the concentration of Pt to 1% played a key role in developing bactericidal effect, since the fabrics coated with colloids containing Pt 0.1% allowed the growth of bacteria colonies (Fig. S2). The plausible mechanism behind the observed antibacterial activity can be the role of Pt ions in interactions with the thiol groups in bacteria cell membrane, which damaged the cell wall and killed the bacteria (Tahir et al. 2017). It has also been reported that platinum can interact with DNA, and respiratory mechanisms of bacteria cell, preventing their proliferation (Tahir et al. 2017).

UV protection of fabrics

Measuring the UPF level of fabrics showed that applying the synthesised binary TiO_2/Pt colloids to fabrics enhanced their UV protection property (Fig. 13). However, adding silica to the coating formulation reduced the overall UPF level. Also, increasing the concentration of Pt resulted in increasing the UPF level for both groups of fabrics coated with ternary and binary colloids. Increased UV protection

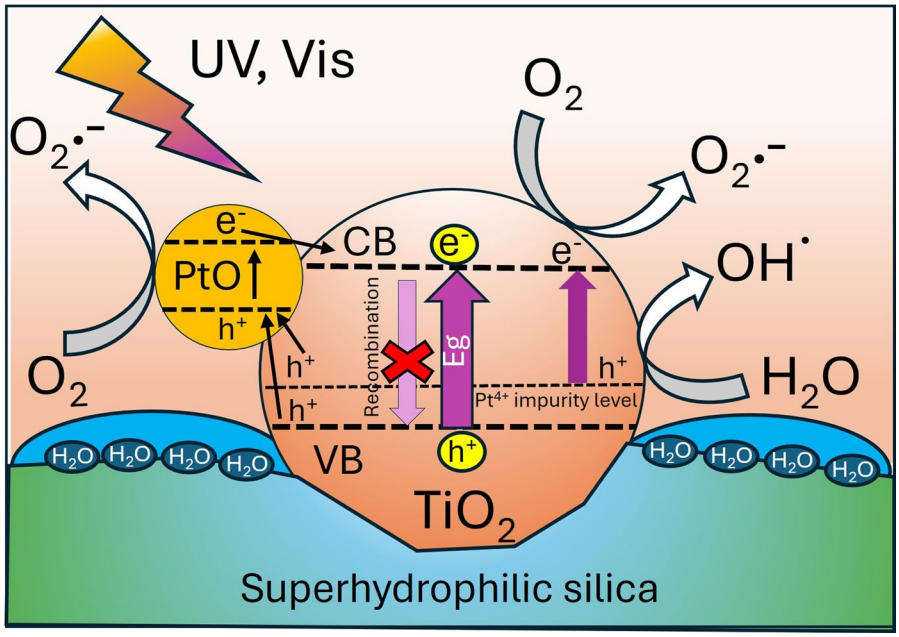

Fig. 11 The proposed mechanisms for photocatalytic activity of self-cleaning TiO_2/Pt/SiO_2 coating under UV and visible light

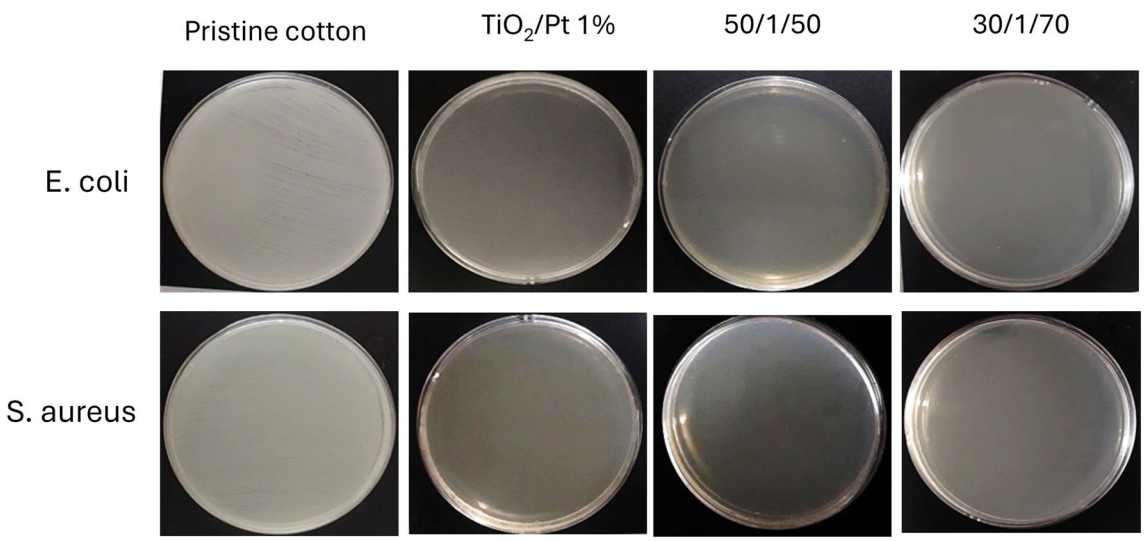

Fig. 12 The antibacterial activity of cotton fabric coated with Pt-modified colloids

of fabrics is related to the intrinsic light absorption properties of pure and modified TiO_2 nanoparticles. Under UV irradiation, TiO_2 generates pairs of electrons and holes, which on the one hand can initiate the redox reactions on the surface of photocatalysts and produce a self-cleaning effect on fabric (Schneider et al. 2014). But on the other hand, these pairs may be recombined and release their absorbed energy in the form of heat (Schneider et al. 2014). This phenomenon gives rise to a UV protection property on the coated surface (Yang et al. 2004). The increased UPF level after incorporating Pt can be related to the modified optical properties of TiO_2 nanoparticles or the presence of Pt on the surface of fabrics. Silica reduced the overall UV protection of fabrics, due to its antireflective properties which in turn increased the UV transmittance through the fabrics (Pakdel et al. 2015b). Testing the washing fastness of fabrics revealed that the presence of Pt resulted in a more durable UV protection property on fabrics which can be attributed to the penetration of Pt-containing nanocomposites into the structure of cellulose and the attachment of doped colloids to the surface of fabrics. Figure 13f depicts the SEM image of the sample after 10 wash cycles, showing the presence of applied coatings on the fibre. The detection of Ti, Si, and Pt element signals in the XPS analysis of the washed sample further corroborated the washing fastness of the applied coating (Fig. 13g-i).

Mechanical properties of fabrics

The effects of coating process on mechanical properties of cotton fabric were investigated based on the measured breaking loads, bending rigidity, and air permeability (Fig. 14). Figure 14a demonstrated that the deposition of pure TiO_2 and TiO_2/Pt/SiO_2 colloids increased the breaking loads of fabrics in both warp and weft directions which can be due to the role of applied coatings in increasing the diameter of fibres. It can also be realised that the treatment of fabrics in acidic colloids did not cause any degradation in fibres and deterioration of their mechanical strength. The stiffness of fabrics was compared based on the bending modulus values (Fig. 14b), and it was observed that applying pure TiO_2 increased the stiffness of fabrics by up to 65.4% and 24.8% in warp and weft directions respectively. After incorporating silica into the coating formulation, the bending modulus of fabric changed by 183.7% and 62.3% in warp and weft directions, respectively, compared with the pristine fabric. This can be related to the deposition of nanoparticles on fibres surface and binding them together, preventing their free movement and their bending behaviour under their own weight. Testing the air-permeability of fabrics revealed that the applied coatings slightly reduced the air permeability of fabrics (Fig. 14c). This was related to the deposition of

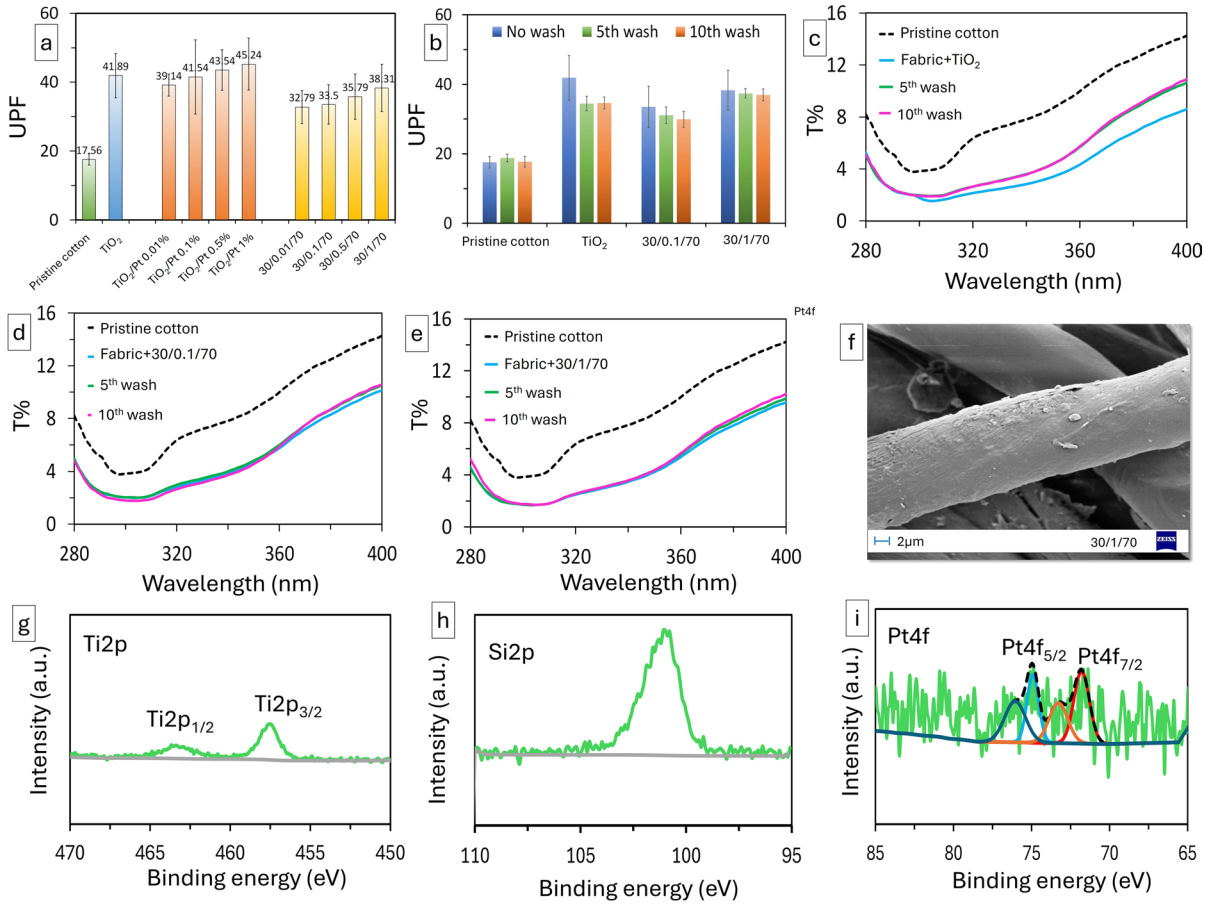

Fig. 13 (**a**) UV protection of coated fabrics; (**b**) washing fastness of coated fabrics; (**c**-**e**) the variation of UV transmittance through fabrics after 10 washing cycles; (**f**) The SEM image of a cotton fibre coated with 30/1/70 colloid after 10 washing cycles; (**g**-**i**) XPS analysis of the sample coated with 30/1/70 colloid after 10 washing cycles (The dashed line represents the simulated graph based on the deconvoluted curves)

nanoparticles in the pores within the structure of fabrics, reducing the free air passage.

Conclusion

Two main groups of colloids including TiO_2/Pt and TiO_2/Pt/SiO_2 colloids were synthesised and applied to fabrics with the aim of evaluating the role of silica and Pt in imparting self-cleaning property, antibacterial activity and UV protection to cotton fabrics. The colloids were synthesised via a low temperature sol–gel method using different molar concentrations of Pt and silica including Pt:Ti 0.01%, 0.1, 0.5%, 1%, and TiO_2/SiO_2 50/50 and 30/70, and applied to cotton fabrics via a dip-pad-dry-cure method. The obtained results confirmed the role of Pt dopant in enhancing the visible-light-induced photocatalytic activity of superhydrophilic coated fabrics. Its effect on enhancing the self-cleaning property of fabrics became synergistically noticeable after including the silica into the coating formulation based on the ratio of TiO_2/SiO_2 30/70. The fabrics coated with the TiO_2/Pt/SiO_2 30/1/70 colloid were superhydrophilic and showed the best self-cleaning property under both UV and visible light. XPS analysis confirmed the successful incorporation of Pt^{4+} ions into the lattice of anatase TiO_2 and the self-doping of TiO_2 with Ti^{3+}. These factors, combined with the superhydrophilicity of the fabrics, played key roles in

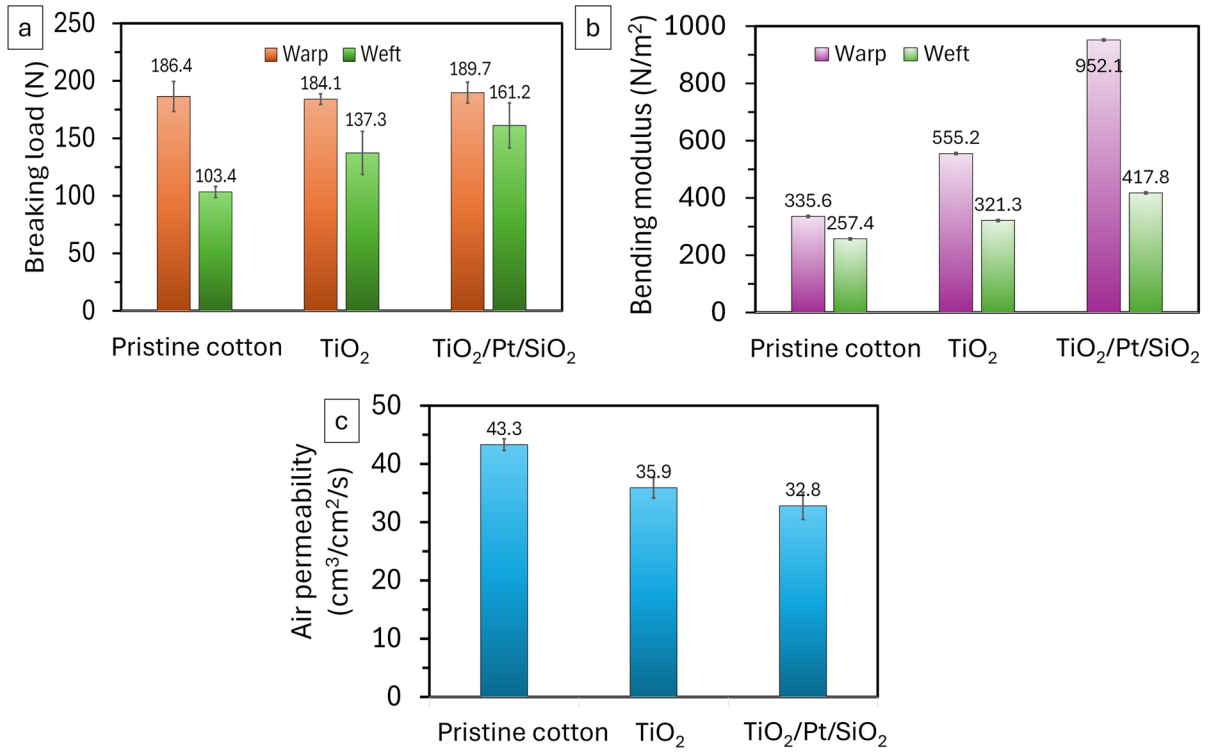

Fig. 14 Mechanical properties of cotton samples before and after treatment with TiO_2 and $TiO_2/Pt/SiO_2$ 50/1/50 colloids, a) breaking load, b) bending modulus, and c) air permeability

enhancing the visible-light-induced photocatalytic activity of the developed coatings. Moreover, it was demonstrated that the fabrics coated with TiO_2/Pt and $TiO_2/Pt/SiO_2$ colloids (Pt:Ti 1%) possessed a 100% bactericidal functionality against *E. coli* and *S. aureus* bacteria. The doping process and increasing the concentration of Pt to 1% increased the UV protection level of coated fabrics to the excellent level of 45 + , while the addition of silica reduced it. The applied $TiO_2/Pt/SiO_2$ 30/1/70 coating showed a great washing fastness and withstood up to 10 accelerated wash cycles. The findings of this study provided new insights on the synergistic effects of Pt and SiO_2 on improving the photocatalytic activity of TiO_2 nanoparticles, which can be utilised in developing novel functional coatings with enhanced features.

Acknowledgments The authors wish to acknowledge research support from the Research Centre of Textiles for Future Fashion, the Hong Kong Polytechnic University.

Authors contributions E. P. Conceptualisation, Methodology, Investigation, Writing—original draft, Data curation WA. D. Supervision, methodology, Writing-review & editing S. K. Data curation, Investigation M. P. G. Data curation, Investigation X. W. Supervision, Writing—review & editing All authors reviewed the manuscript.

Funding Open access funding provided by The Hong Kong Polytechnic University. This work was partially supported by the Research Centre of Textiles for Future Fashion at The Hong Kong Polytechnique University.

Data availability No datasets were generated or analysed during the current study.

Declarations

Conflict of interest The authors declare no competing interests.

Consent for publication All authors agreed to the publication in the submitted form.**Ethical approval.**Not applicable.

References

Abidi N, Manike M (2018) X-ray diffraction and FTIR investigations of cellulose deposition during cotton fiber development. Text Res J 88(7):719–730. https://doi.org/10.1177/0040517516688634

Abidi N, Hequet E, Tarimala S, Dai LL (2007) Cotton fabric surface modification for improved UV radiation protection using sol–gel process. J Appl Polym Sci 104(1):111–117. https://doi.org/10.1002/app.24572

Abidi N, Hequet E, Cabrales L, Gannaway J, Wilkins T, Wells LW (2008) Evaluating cell wall structure and composition of developing cotton fibers using Fourier transform infrared spectroscopy and thermogravimetric analysis. J Appl Polym Sci 107(1):476–486. https://doi.org/10.1002/app.27100

Abidi N, Cabrales L, Haigler CH (2014) Changes in the cell wall and cellulose content of developing cotton fibers investigated by FTIR spectroscopy. Carbohyd Polym 100:9–16. https://doi.org/10.1016/j.carbpol.2013.01.074

Abualnaja KM, ElAassar MR, Ghareeb RY, Ibrahim AA, Abdelsalam NR (2021) Development of photo-induced Ag^0/TiO_2 nanocomposite coating for photocatalysis, self-cleaning and antimicrobial polyester fabric. J Market Res 15:1513–1523. https://doi.org/10.1016/j.jmrt.2021.08.127

Bai W, Pakdel E, Wang Q, Tang B, Wang J, Chen Z, Zhang Y, Hurren C, Wang X (2022) Synergetic Adsorption-Photocatalysis Process of Titania-Silica Photocatalysts and their Immobilization on PEEK Nonwoven Filter for VOC Removal. J Environ Chem Eng 10(6):108920. https://doi.org/10.1016/j.jece.2022.108920

Behzadnia, A., Montazer, M., Mahmoudi Rad, M., & Rastgoo, M. (2024). Fabrication of multifunctional wool textile using the synthesis of silver-modified N-doped ZnO/TiO₂ photocatalysts. Heliyon, 10(16). https://doi.org/10.1016/j.heliyon.2024.e36522

Bharti B, Kumar S, Lee H-N, Kumar R (2016) Formation of oxygen vacancies and Ti^{3+} state in TiO_2 thin film and enhanced optical properties by air plasma treatment. Sci Rep 6(1):32355. https://doi.org/10.1038/srep32355

Bharti B, Li H, Liu D, Kumar H, Manikandan V, Zha X, Ouyang F (2020) Efficient Zr-doped FS–TiO_2/SiO_2 photocatalyst and its performance in acrylonitrile removal under simulated sunlight. Appl Phys A 126(11):887. https://doi.org/10.1007/s00339-020-04066-4

Bingham S, Daoud WA (2011) Recent Advances in Making Nano-sized TiO_2 Visible-Light Active Through Rare-Earth Metal Doping. J Mater Chem 21(7):2041–2050. https://doi.org/10.1039/C0JM02271C

Bumajdad, A., & Madkour, M. (2014). Understanding the superior photocatalytic activity of noble metals modified titania under UV and visible light irradiation [https://doi.org/10.1039/C3CP54411G]. *Physical Chemistry Chemical Physics*, *16*(16), 7146–7158. https://doi.org/10.1039/C3CP54411G

Choi J, Park H, Hoffmann MR (2010) Effects of Single Metal-Ion Doping on the Visible-Light Photoreactivity of TiO_2. The Journal of Physical Chemistry C 114(2):783–792. https://doi.org/10.1021/jp908088x

Drelich, J., Chibowski, E., Meng, D. D., & Terpilowski, K. (2011). Hydrophilic and superhydrophilic surfaces and materials. *Soft Matter*, *7*(21), 9804–9828. https://doi.org/10.1039/C1SM05849E

Feng C, Wang Y, Zhang J, Yu L, Li D, Yang J, Zhang Z (2012) The effect of infrared light on visible light photocatalytic activity: An intensive contrast between Pt-doped TiO2 and N-doped TiO2. Appl Catal B 113–114:61–71. https://doi.org/10.1016/j.apcatb.2011.09.027

Gashti, M. P., Pakdel, E., & Alimohammadi, F. (2016). Nanotechnology-based Coating Techniques for Smart Textiles. In J. Hu (Ed.), *Active Coatings for Smart Textiles* (pp. 243–268). Woodhead Publishing. https://doi.org/10.1016/B978-0-08-100263-6.00011-3

Gayle AJ, Lenef JD, Huff PA, Wang J, Fu F, Dadheech G, Dasgupta NP (2022) Visible-Light-Driven Photocatalysts for Self-Cleaning Transparent Surfaces. Langmuir 38(38):11641–11649. https://doi.org/10.1021/acs.langmuir.2c01455

Hu Y, Song X, Jiang S, Wei C (2015) Enhanced photocatalytic activity of Pt-doped TiO2 for NOx oxidation both under UV and visible light irradiation: A synergistic effect of lattice Pt4+ and surface PtO. Chem Eng J 274:102–112. https://doi.org/10.1016/j.cej.2015.03.135

Kim S, Hwang S-J, Choi W (2005) Visible Light Active Platinum-Ion-Doped TiO2 Photocatalyst. J Phys Chem B 109(51):24260–24267. https://doi.org/10.1021/jp055278y

Krishnan P, Liu M, Itty PA, Liu Z, Rheinheimer V, Zhang M-H, Monteiro PJM, Yu LE (2017) Characterization of photocatalytic TiO_2 powder under varied environments using near ambient pressure X-ray photoelectron spectroscopy. Sci Rep 7(1):43298. https://doi.org/10.1038/srep43298

Liu L, Corma A (2018) Metal Catalysts for Heterogeneous Catalysis: From Single Atoms to Nanoclusters and Nanoparticles. Chem Rev 118(10):4981–5079. https://doi.org/10.1021/acs.chemrev.7b00776

Liu T, Liang R, Qin W (2023) Anti-fouling TiO_2-Coated Polymeric Membrane Ion-Selective Electrodes with Photocatalytic Self-Cleaning Properties. Anal Chem 95(16):6577–6585. https://doi.org/10.1021/acs.analchem.2c05514

Long M, Zheng L, Tan B, Shu H (2016) Photocatalytic self-cleaning cotton fabrics with platinum (IV) chloride modified TiO2 and N-TiO2 coatings. Appl Surf Sci 386:434–441. https://doi.org/10.1016/j.apsusc.2016.06.056

Maqbool Q, Favoni O, Wicht T, Lasemi N, Sabbatini S, Stöger-Pollach M, Ruello ML, Tittarelli F, Rupprechter G (2024) Highly Stable Self-Cleaning Paints Based on Waste-Valorized PNC-Doped TiO2 Nanoparticles. ACS Catal 14(7):4820–4834. https://doi.org/10.1021/acscatal.3c06203

Méndez FJ, Barrón-Romero D, Pérez O, Flores-Cruz RD, Rojas-Challa Y, García-Macedo JA (2023) A highly efficient and recyclable Pt/TiO2 thin film photocatalytic system for sustainable hydrogen production. Mater Chem Phys 305:127925. https://doi.org/10.1016/j.matchemphys.2023.127925

Milošević M, Radoičić M, Ohara S, Abe H, Spasojević J, Mančić L, Šaponjić Z (2023) Advanced photocatalysis mediated by TiO2/Ag/TiO2 nanoparticles modified cotton fabric. Cellulose 30(7):4749–4771. https://doi.org/10.1007/s10570-023-05165-0

Mohajernia S, Andryskova P, Zoppellaro G, Hejazi S, Kment S, Zboril R, Schmidt J, Schmuki P (2020) Influence of Ti^{3+} defect-type on heterogeneous photocatalytic H_2 evolution activity of TiO_2. Journal of Materials Chemistry A 8(3):1432–1442. https://doi.org/10.1039/C9TA10855F

Mollick S, Repon MR, Haji A, Jalil MA, Islam T, Khan MM (2023) Progress in self-cleaning textiles: parameters, mechanism and applications. Cellulose 30(17):10633–10680. https://doi.org/10.1007/s10570-023-05539-4

Montazer M, Pakdel E (2011) Functionality of nano titanium dioxide on textiles with future aspects: Focus on wool. J Photochem Photobiol, C 12(4):293–303. https://doi.org/10.1016/j.jphotochemrev.2011.08.005

Montazer M, Behzadnia A, Moghadam MB (2012) Superior self-cleaning features on wool fabric using TiO_2/Ag nanocomposite optimized by response surface methodology. J Appl Polym Sci 125(S2):E356–E363. https://doi.org/10.1002/app.36768

Natsathaporn P, Herwig G, Altenried S, Ren Q, Rossi RM, Crespy D, Itel F (2023) Functional Fiber Membranes with Antibacterial Properties for Face Masks. Advanced Fiber Materials 5(4):1519–1533. https://doi.org/10.1007/s42765-023-00291-7

Ni M, Leung MKH, Leung DYC, Sumathy K (2007) A review and recent developments in photocatalytic water-splitting using for hydrogen production. Renew Sustain Energy Rev 11(3):401–425. https://doi.org/10.1016/j.rser.2005.01.009

Nishiyama N, Fujiwara Y, Adachi K, Inumaru K, Yamazaki S (2015) Preparation of porous metal-ion-doped titanium dioxide and the photocatalytic degradation of 4-chlorophenol under visible light irradiation. Appl Catal B 176–177:347–353. https://doi.org/10.1016/j.apcatb.2015.04.015

Pakdel E, Daoud W (2013) Self-cleaning Cotton Functionalized with TiO_2/SiO_2: Focus on the Role of Silica. J Colloid Interface Sci 401:1–7. https://doi.org/10.1016/j.jcis.2013.03.016

Pakdel E, Daoud WA, Sun L, Wang X (2014a) Visible and UV Functionality of TiO_2 Ternary Nanocomposites on Cotton. Appl Surf Sci 321:447–456. https://doi.org/10.1016/j.apsusc.2014.10.018

Pakdel E, Daoud WA, Wang X (2014b) Assimilating the Photo-Induced Functions of TiO_2-based Compounds in Textiles: Emphasis on the Sol-Gel Process. Text Res J 85(13):1404–1428. https://doi.org/10.1177/0040517514551462

Pakdel E, Daoud WA, Afrin T, Sun L, Wang X (2015a) Self-Cleaning Wool: Effect of Noble Metals and Silica on Visible-Light-Induced Functionalities of Nano TiO_2 Colloid. The Journal of the Textile Institute 106(12):1348–1361. https://doi.org/10.1080/00405000.2014.995461

Pakdel E, Daoud WA, Sun L, Wang X (2015b) Reprint of: Photostability of wool fabrics coated with pure and modified TiO2 colloids. J Colloid Interface Sci 447:191–201. https://doi.org/10.1016/j.jcis.2015.01.076

Pakdel E, Daoud WA, Afrin T, Sun L, Wang X (2017) Enhanced Antimicrobial Coating on Cotton and Its Impact on UV Protection and Physical Characteristics. Cellulose 24(9):4003–4015. https://doi.org/10.1007/s10570-017-1374-y

Pakdel E, Daoud WA, Seyedin S, Wang J, Razal JM, Sun L, Wang X (2018) Tunable Photocatalytic Selectivity of TiO_2/SiO_2 Nanocomposites: Effect of Silica and Isolation Approach. Colloids Surf, A 552:130–141. https://doi.org/10.1016/j.colsurfa.2018.04.070

Pakdel E, Wang J, Kashi S, Sun L, Wang X (2020) Advances in Photocatalytic Self-Cleaning, Superhydrophobic and Electromagnetic Interference Shielding Textile Treatments. Adv Coll Interface Sci 277:102116. https://doi.org/10.1016/j.cis.2020.102116

Pakdel E, Daoud WA, Varley RJ, Wang X (2022) Antibacterial Textile and The Effect of Incident Light Wavelength on Its Photocatalytic Self-Cleaning Activity. Mater Lett 318:132223. https://doi.org/10.1016/j.matlet.2022.132223

Pakdel E, Sharp J, Kashi S, Bai W, Gashti MP, Wang X (2023) Antibacterial Superhydrophobic Cotton Fabric with Photothermal, Self-Cleaning, and Ultraviolet Protection Functionalities. ACS Appl Mater Interfaces 15(28):34031–34043. https://doi.org/10.1021/acsami.3c04598

Pakdel E, Daoud WA, Wang X (2024a) Effect of the Photoreduction Process on the Self-Cleaning and Antibacterial Activity of Au-Doped TiO_2 Colloids on Cotton Fabric. ACS Appl Mater Interfaces 16(19):25221–25235. https://doi.org/10.1021/acsami.4c01238

Pakdel E, Kashi S, Sharp J, Wang X (2024b) Superhydrophobic, Antibacterial, and EMI Shielding Properties of Ag/PDMS-Coated Cotton Fabrics. Cellulose 31:3921–3946. https://doi.org/10.1007/s10570-024-05819-7

Pelaez, M., Nolan, N. T., Pillai, S. C., Seery, M. K., Falaras, P., Kontos, A. G., Dunlop, P. S. M., Hamilton, J. W. J., Byrne, J. A., O'Shea, K., Entezari, M. H., & Dionysiou, D. D. (2012). A review on the visible light active titanium dioxide photocatalysts for environmental applications. Applied Catalysis B: Environmental, 125(Supplement C), 331–349. https://doi.org/10.1016/j.apcatb.2012.05.036

Post P, Wurlitzer L, Maus-Friedrichs W, Weber AP (2018) Characterization and Applications of Nanoparticles Modified in-Flight with Silica or Silica-Organic Coatings. Nanomaterials 8(7):530. https://doi.org/10.3390/nano8070530

Ren X-N, Hu Z-Y, Jin J, Wu L, Wang C, Liu J, Liu F, Wu M, Li Y, Tendeloo GV, Su B-L (2017) Cocatalyzing Pt/PtO Phase-Junction Nanodots on Hierarchically Porous TiO_2 for Highly Enhanced Photocatalytic Hydrogen Production.

ACS Appl Mater Interfaces 9(35):29687–29698. https://doi.org/10.1021/acsami.7b07226

Romero-Morán A, Sánchez-Salas JL, Molina-Reyes J (2021) Influence of selected reactive oxygen species on the photocatalytic activity of TiO_2/SiO_2 composite coatings processed at low temperature. Appl Catal B 291:119685. https://doi.org/10.1016/j.apcatb.2020.119685

Rosario AV, Pereira EC (2014) The role of Pt addition on the photocatalytic activity of TiO_2 nanoparticles: The limit between doping and metallization. Appl Catal B 144:840–845. https://doi.org/10.1016/j.apcatb.2013.07.029

Schneider J, Curti M (2023) Spectroscopic and kinetic characterization of photogenerated charge carriers in photocatalysts. Photochem Photobiol Sci 22(1):195–217. https://doi.org/10.1007/s43630-022-00297-x

Schneider J, Matsuoka M, Takeuchi M, Zhang J, Horiuchi Y, Anpo M, Bahnemann DW (2014) Understanding TiO_2 Photocatalysis: Mechanisms and Materials. Chem Rev 114(19):9919–9986. https://doi.org/10.1021/cr5001892

Sun Y, Mwandeje JB, Wangatia LM, Zabihi F, Nedeljković J, Yang S (2020) Enhanced Photocatalytic Performance of Surface-Modified TiO_2 Nanofibers with Rhodizonic Acid. Advanced Fiber Materials 2(2):118–122. https://doi.org/10.1007/s42765-020-00037-9

Tahir K, Nazir S, Ahmad A, Li B, Khan AU, Khan ZUH, Khan FU, Khan QU, Khan A, Rahman AU (2017) Facile and green synthesis of phytochemicals capped platinum nanoparticles and in vitro their superior antibacterial activity. J Photochem Photobiol, B 166:246–251. https://doi.org/10.1016/j.jphotobiol.2016.12.016

Tang B, Zhang M, Hou X, Li J, Sun L, Wang X (2012) Coloration of Cotton Fibers with Anisotropic Silver Nanoparticles. Ind Eng Chem Res 51(39):12807–12813. https://doi.org/10.1021/ie3015704

Tomšič, B., Ofentavšek, L., & Fink, R. (2024). Toward sustainable household laundry. Washing quality vs. environmental impacts. *International Journal of Environmental Health Research*, *34*(2), 1011–1022. https://doi.org/10.1080/09603123.2023.2194615

van Deelen TW, Hernández Mejía C, de Jong KP (2019) Control of metal-support interactions in heterogeneous catalysts to enhance activity and selectivity. Nat Catal 2(11):955–970. https://doi.org/10.1038/s41929-019-0364-x

Vikrant K, Weon S, Kim K-H, Sillanpää M (2021) Platinized titanium dioxide (Pt/TiO2) as a multi-functional catalyst for thermocatalysis, photocatalysis, and photothermal catalysis for removing air pollutants. Appl Mater Today 23:100993. https://doi.org/10.1016/j.apmt.2021.100993

Wang J, Zhao J, Sun L, Wang X (2015) A review on the application of photocatalytic materials on textiles. Text Res J 85(10):1104–1118. https://doi.org/10.1177/0040517514559583

Wang X, Noman MT, Petrů M, Kang G (2024) Enhancing dynamic viscoelastic performance of flax fiber/fly ash hollow cenosphere-reinforced composites coated by in situ fabrication of ultrasonically synthesized nanotitanium dioxide. J Appl Polym Sci 141(33):e55843. https://doi.org/10.1002/app.55843

Wang, Q., Bai, W., Lu, X., Wang, J., Pakdel, E., Yu, Z., Cui, Y., & Liu, Q. (2023). Thermally oxidized PAN as photocatalyst support layer for VOCs removal. *The Journal of The Textile Institute*, *115*(8), 1362–1370. https://doi-org.ezproxy.lb.polyu.edu.hk/https://doi.org/10.1080/00405000.2023.2240058

Wei, Y., Wu, Q., Meng, H., Zhang, Y., & Cao, C. (2023). Recent advances in photocatalytic self-cleaning performances of TiO_2-based building materials [https://doi.org/10.1039/D2RA07839B]. *RSC Advances*, *13*(30), 20584–20597. https://doi.org/10.1039/D2RA07839B

Wolek ATY, Hicks KE, Notestein JM (2023) Tuning acidity in silica-overcoated oxides for hydroalkoxylation. J Catal 426:113–125. https://doi.org/10.1016/j.jcat.2023.06.008

Wu Z, Sheng Z, Liu Y, Wang H, Mo J (2011) Deactivation mechanism of PtO_x/TiO_2 photocatalyst towards the oxidation of NO in gas phase. J Hazard Mater 185(2):1053–1058. https://doi.org/10.1016/j.jhazmat.2010.10.013

Xie W, Pakdel E, Liang Y, Liu D, Sun L, Wang X (2020) Natural Melanin/TiO_2 Hybrids for Simultaneous Removal of Dyes and Heavy Metal Ions Under Visible Light. J Photochem Photobiol, A 389:112292. https://doi.org/10.1016/j.jphotochem.2019.112292

Xiu Z, Guo M, Zhao T, Pan K, Xing Z, Li Z, Zhou W (2020) Recent advances in Ti^{3+} self-doped nanostructured TiO_2 visible light photocatalysts for environmental and energy applications. Chem Eng J 382:123011. https://doi.org/10.1016/j.cej.2019.123011

Xue, D., Luo, J., Li, Z., Yin, Y., & Shen, J. (2020). Enhanced Photoelectrochemical Properties from Mo-Doped TiO_2 Nanotube Arrays Film. *Coatings*, *10*(1), 75. https://www.mdpi.com/2079-6412/10/1/75

Yang H, Zhu S, Pan N (2004) Studying the Mechanisms of Titanium Dioxide as Ultraviolet-Blocking Additive for Films and Fabrics by an Improved Scheme. J Appl Polym Sci 92(5):3201–3210. https://doi.org/10.1002/app.20327

Yang J-L, Wang H-J, Qi X, Zheng Q-N, Tian J-H, Zhang H, Li J-F (2024) Understanding the Behaviors of Plasmon-Induced Hot Carriers and Their Applications in Photocatalysis. ACS Appl Mater Interfaces 16(10):12149–12160. https://doi.org/10.1021/acsami.4c00709

Yu H, Xiao P, Tian J, Wang F, Yu J (2016) Phenylamine-Functionalized rGO/TiO_2 Photocatalysts: Spatially Separated Adsorption Sites and Tunable Photocatalytic Selectivity. ACS Appl Mater Interfaces 8(43):29470–29477. https://doi.org/10.1021/acsami.6b09903

Zang W, Lee J, Tieu P, Yan X, Graham GW, Tran IC, Wang P, Christopher P, Pan X (2024) Distribution of Pt single atom coordination environments on anatase TiO_2 supports controls reactivity. Nat Commun 15(1):998. https://doi.org/10.1038/s41467-024-45367-z

Zhai H, Liu Z, Xu L, Liu T, Fan Y, Jin L, Dong R, Yi Y, Li Y (2022) Waste Textile Reutilization Via a Scalable Dyeing Technology: A Strategy to Enhance Dyestuffs Degradation Efficiency. Advanced Fiber Materials 4(6):1595–1608. https://doi.org/10.1007/s42765-022-00192-1

Zhang W, He H, Li H, Duan L, Zu L, Zhai Y, Li W, Wang L, Fu H, Zhao D (2021) Visible-Light Responsive TiO2-Based Materials for Efficient Solar Energy Utilization. Adv Energy Mater 11(15):2003303. https://doi.org/10.1002/aenm.202003303

Zhang J, Wang X, Shen K, Lu W, Wang J, Chen F (2023a) Defect Engineering in g-C_3N_4 Quantum-Dot-Modified TiO_2 Nanofiber: Uncovering Novel Mechanisms for the Degradation of Tetracycline in Coexistence with Cu^{2+}. Advanced Fiber Materials 5(1):168–182. https://doi.org/10.1007/s42765-022-00205-z

Zhang L, Leung MY, Boriskina S, Tao X (2023b) Advancing life cycle sustainability of textiles through technological innovations. Nature Sustainability 6(3):243–253. https://doi.org/10.1038/s41893-022-01004-5

Zhao J, Wang J, Fan L, Pakdel E, Huang S, Wang X (2017) Immobilization of Titanium Dioxide on PAN Fiber as a Recyclable Photocatalyst via Co-dispersion Solvent Dip Coating. Text Res J 87(5):570–581. https://doi.org/10.1177/0040517516632479

Zhou D, Luo H, Zhang F, Wu J, Yang J, Wang H (2022) Efficient Photocatalytic Degradation of the Persistent PET Fiber-Based Microplastics over Pt Nanoparticles Decorated N-Doped TiO_2 Nanoflowers. Advanced Fiber Materials 4(5):1094–1107. https://doi.org/10.1007/s42765-022-00149-4

Zhou B, Zhao X, Liu Y (2024) The latest research progress on the antibacterial properties of TiO 2nanocomposites. J The Textile Institute. https://doi.org/10.1080/00405000.2024.2349324